Landslide_characterization_in_the_Polog_region_by_innovative_and_conventional_methods, RIVISTA ITALIANA DI GEOTECNICA 4/2021 dx

Article *in* Rivista Italiana di Geotecnica · August 2022

DOI: 10.19199/2021.4.0557-1405.007

CITATIONS
0

READS
62

8 authors, including:

Milorad Jovanovski
Ss. Cyril and Methodius University in Skopje
180 PUBLICATIONS **244** CITATIONS
SEE PROFILE

Igor Peshevski
Ss. Cyril and Methodius University in Skopje
103 PUBLICATIONS **420** CITATIONS
SEE PROFILE

Gjirgji Gjorgjiev
Ss. Cyril and Methodius University in Skopje
3 PUBLICATIONS **1** CITATION
SEE PROFILE

Natasha Nedelkovska
Ss. Cyril and Methodius University in Skopje
16 PUBLICATIONS **12** CITATIONS
SEE PROFILE

Landslide characterization in the Polog Region (R.N. Macedonia) by innovative and conventional methods

Milorad Jovanovski,* Igor Peshevski,* Gjorgi Gjorgiev,* Natasha Nedelkovska,**
Gianfranco Nicodemo,*** Diego Reale,**** Gianfranco Fornaro,**** Dario Peduto***

Summary

The paper presents the preliminary results of an ongoing international multidisciplinary project funded by the United Nations Development Programme (UNDP) over the Polog Region in R.N. Macedonia. The combined effects of a complex geological setting, an articulate morphology and particular climate conditions make the Polog Region one of the most landslide-prone areas in the country. Over the study area (extending for approximately 1000 km^2), preliminary landslide susceptibility studies were performed; however, the extent of landslide hazard in the region needs to be understood to a higher level of detail. The aim of the project is to detect critical sediment sources in the Polog Region and propose technical measures – at a feasibility study level – for the areas exposed to the highest hazard level. In the first stage, via the joint contribution of geologists/geomorphologists, hydrologists, geotechnical and hydraulic engineers, the activities focused on the preparation of thematic sediment source maps, among which the landslide inventory is of highest importance.

Preliminarily, base activities entailed i) the analysis of old and recent geological and topographic maps as well as technical reports on past landslides, ii) field surveys, and iii) the collection of witnesses to particular landslide events.

The collected data were then analyzed in combination with wide-area airborne LIDAR (Light Detection and Ranging) and displacement measurements by means of satellite multipass Synthetic Aperture Radar Differential Interferometry (DInSAR), which was applied for the first time in this region for such a purpose. Preliminary landslide susceptibility analyses were also carried out in GIS environment.

The followed approach proved to be satisfactory for a feasibility study level when base and thematic maps are incomplete or lacking. The obtained results allowed i) gathering an overview of the unstable conditions affecting the slopes of Polog Region and ii) detecting the most landslide-prone areas, wherein more detailed studies should be addressed in the following stages of the project.
Keywords: landslides, detection, mapping, kinematics, susceptibility, DInSAR

1. Introduction

In the last decades of the twentieth century, the expansion of settlements, rapid urbanization and global climate change caused a considerable increasing of geohazards [Schuster and Highland, 2001]. Landslides are among the most significant and widespread ones, producing enormous social and economic losses worldwide [Kjekstad and Highland, 2009; Herrera *et al.*, 2018].

Studies and investigations pursuing landslide characterization are the necessary background to identify both predisposing and triggering factors useful for qualitative/quantitative risk assessment activities aimed at predicting and mitigating the associated consequences [Fell *et al.*, 2008; Corominas *et al.*, 2014]. In particular, the knowledge on geometric-kinematic features of the landslide-affected area coupled with the analysis of the interaction with the exposed elements can help developing more sophisticated numerical analyses, should the hydro-mechanical soil properties and the groundwater regimen be adequately defined [Cotecchia *et al.,* 2016; Merodo *et al.*, 2014; Sangirardi *et al.*, 2020].

Selecting the appropriate procedure for hazard and risk assessment depends on a number of key factors such as *i)* the scale of analysis (*e.g.* regional, local or site specific) [Fell *et al.*, 2008], *ii)* the purpose of the analysis (*e.g.* emergency, scientific, prevention, control) [Abolmasov *et al.*, 2015; Antronico *et al.*, 2015; Barla *et al.,* 2010; Borrelli *et al.,* 2014; Pilot, 1984; Yin *et al.* 2010], *iii)* the geo-environmental context (*e.g.* primarily natural or predominantly urban-

* Faculty of Civil Engineering of the Ss. Cyril and Methodius University, Skopje, R.N. Macedonia
** Geohydroconsulting Ltd. Skopje, R.N. Macedonia
*** Department of Civil Engineering, University of Salerno, Italy
**** Institute for the Electromagnetic Sensing of the Environment, National Research Council (IREA-CNR), Naples, Italy

 dx.doi.org/10.19199/2021.4.0557-1405.007

ized) [Bonci *et al.*, 2010; Booth *et al.,* 2015; Cascini *et al.,* 2006; Ciampalini *et al.,* 2012; Peduto *et al.,* 2021a].

The geometric and kinematic characterization of mass movements affecting a given area is fundamental [Antronico *et al.,* 2013; Baldi *et al.*, 2008; Carter and Bentley, 1985; Eberhardt, 2008; Grana and Tommasi, 2014; Gullà *et al.,* 2017; Maiorano *et al.,* 2015; Vaunat and Leroueil, 2002] and it can be performed via various methods widely described in the scientific literature [Di Maio *et al.*, 2013; Komac *et al.,* 2015; Massey *et al.*, 2013; Yin *et al.,* 2010]. In particular, among the most used methods, Gullà *et al.* [2017] identify *i)* the geological/geomorphological (GeoG) one, which is mostly effective on a regional scale or over large areas, *ii)* the geotechnical (Geot) one, which is essential when working at slope scale, *iii)* satellite radar images (Sat), which have been successfully used in monitoring urbanized areas that are affected by slow-moving landslides [Peduto *et al.*, 2019b, 2021b; Noviello *et al.*, 2020].

As for GeoG, a geological map of the study area is fundamental for the study of slope instability. In such case, a detailed geological survey, supported by a preliminary photointerpretation analysis, constitutes the first step in the definition of the geological and structural features, and of the geological model of the study area as well. Stereoscopic analysis of aerial photos taken at different times allows for the reconstruction of landslide movements in a study area [Walstra *et al.,* 2007]. However, this operation can be limited by, among other factors, the type of movement, the changes in the vegetation cover resulting even more difficult in urban areas [Guzzetti *et al.*, 2012]. In this regard, field surveys are useful for mapping landslide events immediately after activation/reactivation and for improving or validating the inventory maps obtained from the interpretation of aerial photographs [Guzzetti *et al.,* 2012]. With reference to slow-moving landslides, field surveys aimed at recording cracks and deformations of buildings and infrastructures can reveal slope instabilities [Antronico *et al.*, 2015; Nappo *et al.,* 2019]. In particular, multi-temporal photo comparison of building damage can support the identification of landslide boundary and the landslide activity definition, otherwise not easily mapped through aerial photographs for this type of phenomena. To this aim, nowadays Google Earth imagery (when available) can provide a valuable contribution [Ferlisi *et al.,* 2020; Peduto *et al.,* 2017a].

Integrated geotechnical monitoring networks for the measurement of both surficial and deep displacements can contribute to the geometric and kinematic characterization of unstable sloping areas and support modelling [Cotecchia *et al.,* 2016; Petley *et al.,* 2005; Tommasi *et al.,* 2006]. However, over large areas conventional monitoring can lack cost-effectiveness, most of all when monitoring plans are not included in a general framework. Furthermore, in urban areas, they can be somehow limited by the configurations of buildings and roads. For instance, as for surface displacement monitoring via GPS systems in urban areas, frequent constraints include [Gullà *et al.*, 2017] *i)* vegetation that may disturb the GPS signal reception, *ii)* difficult access to specific sites [Bonci *et al.,* 2010; Gili *et al.,* 2000], *iii)* correct positioning of fixed benchmarks, *iv)* contiguous urban fabric with significant gradients. Even further limitations can be encountered when monitoring deep displacements by inclinometers (*e.g.* presence of underground utility lines, proper positioning of the inclinometer verticals for both sliding surface detection and to kinematic feature retrieval) [Stark and Choi, 2008; Wang *et al.*, 2014].

The conventional geotechnical monitoring of ground displacements can be valuably complemented by the processing of images acquired by spaceborne Synthetic Aperture Radar sensors and processed with advanced multipass Differential Interferometric (DInSAR) techniques. Up to day, the scientific literature reports a number of case studies that successfully investigated potential and limits of the DInSAR techniques for earthquakes [Reale *et al.,* 2011], slow-moving landslides [Bianchini *et al.*, 2013; Calò *et al.,* 2014; Di Maio *et al.,* 2018; Herrera *et al.* 2013; Nicodemo *et al.,* 2020a; Peduto *et al.*, 2018b, 2019b; Tofani *et al.*, 2014; Wasowski and Bovenga, 2014], mining [Crosetto *et al.,* 2005], water extraction [Cigna *et al.*, 2012; Peduto *et al.*, 2015; Sanabria *et al.*, 2014], underground construction works (Bandini *et al.,* 2015) as well as for the monitoring of (infra) structures [Arangio *et al.*, 2013; Fornaro *et al.,* 2013; Infante *et al.*, 2018, 2019; Lanari *et al.*, 2020; Nappo *et al.*, 2019; Nicodemo *et al.*, 2017, 2020b; Peduto *et al.,* 2017b, 2018a, 2017c, 2019a, 2020; Tomás *et al.,* 2013] and for addressing multi-risk issues [Pazzi *et al.,* 2016]. With specific reference to slow-moving landslides, DInSAR data enables investigating past landslide evidences, and creating inventory maps for particular periods [Raspini *et al.*, 2019]. Furthermore, these data provide information on the boundaries and state of activity of the landslide. As for the Balkan area some applications were carried out in Greece by Raucoles *et al.* [2008], Elias *et al.* [2009], in Slovenia by Čarman *et al.* [2014] and within European projects such as Terrafirma (https://www.eurogeosurveys.org/projects/terrafirma/) and PanGeo (www.eurogeosurveys.org/projects/pangeo/).

The territory of R.N. Macedonia (Fig. 1) is severely and frequently hit by landslides, responsible for direct and indirect impacts on the structures, infrastructure and population [Peshevski *et al.*, 2017; Haque *et al.,* 2016]. Results from a recent study on landslide distribution in the country have shown that the northwestern part of the country, more precisely the Polog Region, is the most prone to landsliding processes, primarily triggered by heavy rainfalls and favored by its geological, morphological and tec-

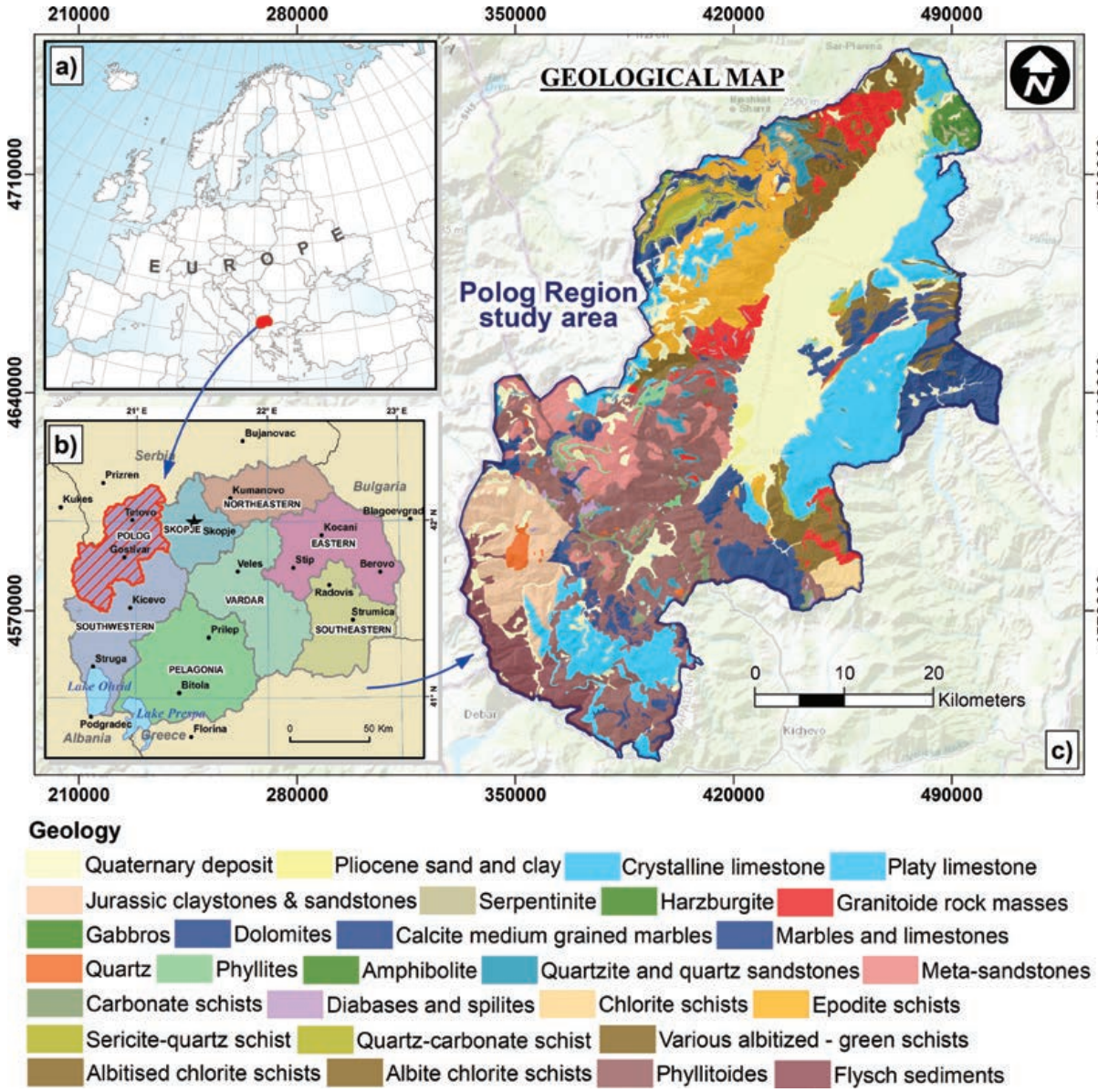

Fig. 1 – Polog Region (R.N. Macedonia) study area: a) location of R.N. Macedonia in Europe; b) location of the Polog Region in R.N. Macedonia country; c) geological map.

Fig. 1 – Area di studio della Regione Polog (R.N. Macedonia): a) ubicazione della R.N. Macedonia in Europa; b) ubicazione della Regione Polog in R.N. Macedonia; c) carta geologica.

tonic setting [PESHEVSKI *et al.* 2019]. Therefore, the necessity for appropriate risk management for this part of the country is urging and landslide susceptibility, hazard and risk assessments are deemed necessary. This means that a landslide inventory of appropriate quality for the region is necessary, in order to perform the proper selection and validation of the susceptibility (or hazard) models and enable systematic approach in the management of the landslide hazard. However, a previous study by PESHEVSKI *et al.* [2019] concluded that complete and accurate inventory – providing insight into the location of landslide phenomena, the type, failure mechanism, triggering factors, frequency of occurrence, volumes and the induced damage [HERVÁS, 2013] – is missing for the Polog Region. Accordingly, the present study aimed at deriving a landslide inventory via the detection and characterization of landslides through *i)* conventional (geological and geomorphological analyses supported by field checks), *ii)* satellite remote sensing DInSAR techniques, *iii)* simplified numerical analyses at regional scale.

The results, together with the analysis of environmental factors, triggering factors and elements at risk will represent the necessary background for more detailed landslide susceptibility, hazard and risk assessment [COROMINAS *et al.,* 2014; VAN WESTEN *et al.,* 2005].

2. Study area: geological context and landsliding

The Polog Region is located in the north-west part of R.N. Macedonia (Fig. 1). It is characterized by mountainous topography and dense hydrographic network comprising torrential streams and rivers, as well as by high population density along the east toe of Shar Planina Mountain and the flat terrain towards the Vardar River.

As for the geological context (Fig. 1c), the study area belongs to the larger regional tectonic unit called Western Macedonian Zone. This unit is represented by rock masses from the Paleozoic, Mesozoic, Pliocene and Quaternary ages. The formation of the terrain itself have begun with the formation of the Paleozoic geosyncline, in the Cambrian and Ordovician. In the lower levels of the Devonian period, marine pelitic and psammitic sediments have been deposited, which have been facies-like altered laterally and vertically. In the upper levels of Devon, the sedimentation has been carried out in a significantly calmer environment when coarse-grained sediments, gravels, sands and clays have been deposited. The end of the Devon is characterized by deposition of carbonate sediments and in some places clastic sediments (sandstones and conglomerates). Towards the end of the Devonian and the beginning of the Carboniferous, the terrain has been affected by Hercynian orogeny, whose movements have manifested by intense regional metamorphism and folding. Primary sediments have been metamorphosed to the extent of green schists and turned into phyllite schists, metasandstones, metaconglomerates, metamorphosed limestones and marbles. In Carboniferous and Permian, certain parts of the former geosynclinal have been under water, where tuffs, limestones, pelite and psammite sediments have been deposited, and rhyolites have been extruded.

The rocks of the green complex of Shar Planina and the carbonate-graphite schists have been deposited in a separate basin that have been formed somewhere after the Permian. The basin has existed until the end of the Middle Triassic in which diabase, tuff, pelite-psamite and carbonate sediments have been deposited in the deeper parts, while in the upper parts of the basin carbonates with cherts have been deposited.

The Triassic is characterized by a dominant deposition of carbonate rocks, which are found in the wider area, and with them the Triassic transgression ends, somewhere towards the beginning of the lower part of the Upper Triassic. At the end of the Triassic there have been strong orogenic movements that have significantly modified the old structures. During the formation of the Jurassic geosynclinal, significant initial magmatism have occurred, and gabbro, diabase, rhyolite, keratorphyre, lamprophyre, granodiorite and granite rocks have been formed. Flysch sediments such as clays, sandstones, marls, marl limestones and limestones with alteration in horizontal and vertical direction have been deposited during the Cretaceous transgression. After the Upper Cretaceous, there have been intense orogenic movements that have formed overthrusts and reverse faults.

At the end of the middle and upper Pliocene, the vertical movements have reached their maximum, thus forming the Polog and Mavrovo grabens. Shar Planina Mountain, as a structure lying in the Alpine orogenic belt, has been significantly elevated by neo-tectonic movements and its high mountain ranges have been affected by glaciation in the Pleistocene. In the Quaternary, especially in the postglacial periods, there have been significant erosion of the surrounding terrains, as well as of the Pliocene sediments, when the formed lakes in the Mavrovo and Polog grabens have been filled, and the Polog lake flowed along the river Vardar, whereas the Mavrovo lake along the rivers Mavrovska reka and Radika. With the retreat of Polog Lake, terraces have been formed, whose sections are present south and southwest of Gostivar. In the peripheral parts of the Polog Region, as a result of torrential rains, large proluvial fans have been formed, and talus on the steep slopes [PETKOVSKI, 1982].

The topographic relief of the Polog study area ranges from 265 to 2700 m above sea level (Fig. 2a) with a complex morphology strongly controlled by the tectonics and geology.

The climate in the Polog Region is hot continental at altitude of 600-900 m a.s.l.; the Shar Planina Mountain has cold continental climate at altitude of 900-1100 m a.s.l. and the remaining area has alpine mountainous climate at altitude over 2250 m a.s.l. Summer is warm and partly wet, winter is cold and snowy, whereas spring and autumn are characterized by rainfalls. In terms of rainfalls, the study area is characterized by the highest annual average rainfall in the country [ILIJOVSKI, 2013]; this ranges from 600 mm/year to more than 1250 mm/year (Fig. 2b). Historically, this region has been exposed to extreme weather conditions and frequent flash flooding.

The geomorphological settings, which mostly depend on the complex geology and tectonics, and the specific hydro-meteorological conditions, are the main predisposing factors for this region to be classified as “landslide-prone”. Over the study area, preliminary landslide susceptibility studies were performed by PESHEVSKI [2015] with some more recent improvements by PESHEVSKI *et al.* [2019], who presented a heuristic approach for preliminary regional landslide susceptibility assessment using limited amount of data. In particular, the authors used an arbitrary polynomial method that takes into account five landslide-conditioning parameters: lithology,

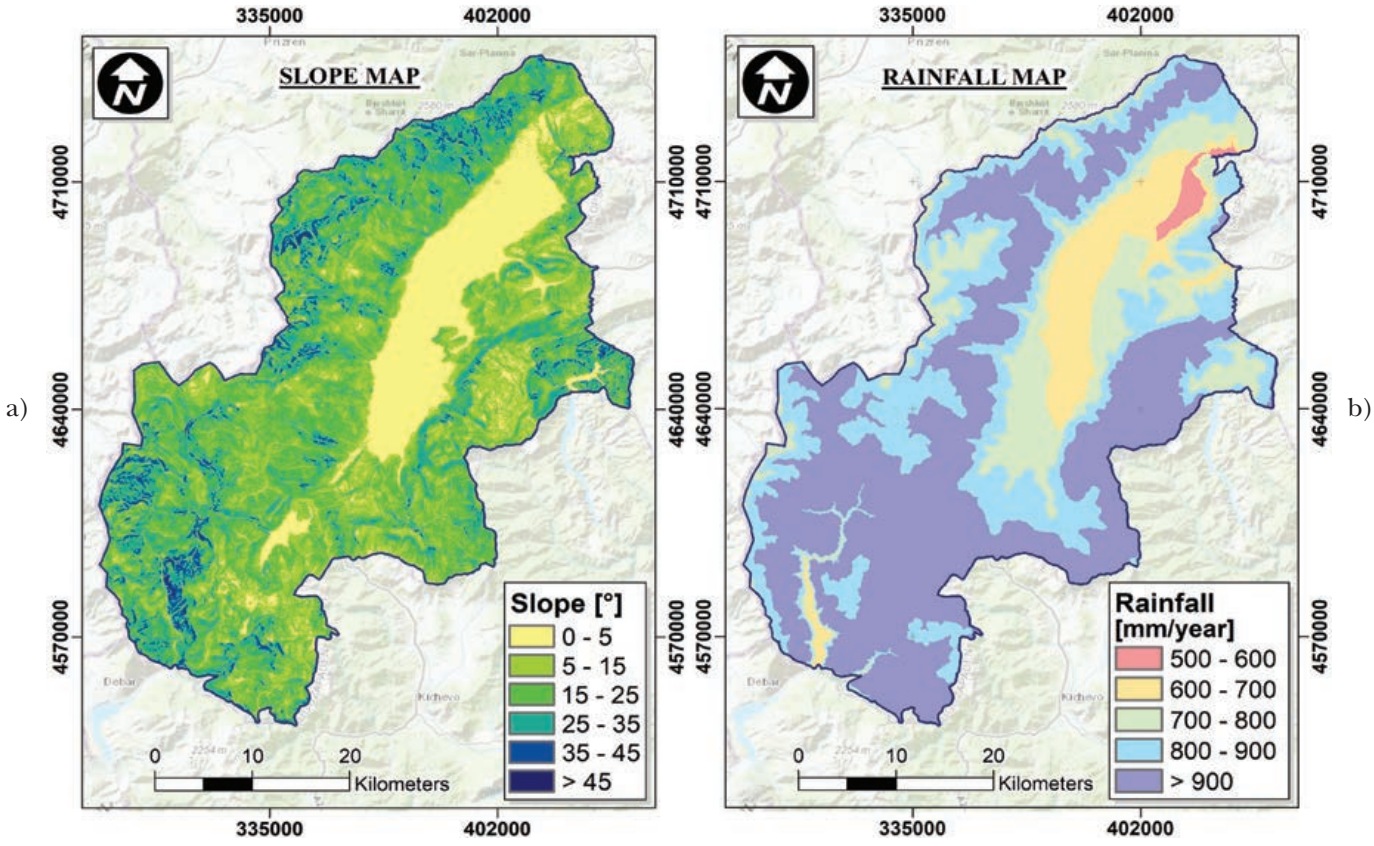

Fig. 2 – a) Slope map and b) rainfall map of the Polog Region.
Fig. 2 – a) Carta delle pendenze e b) Carta delle precipitazioni della Regione Polog.

slope inclination, average annual rainfall, land use and maximum expected seismic intensity. According to the results, a Total Landslide Susceptibility Rating (TLSR) model was obtained by summing the individual rating points of each parameter and dividing the region into five susceptibility zones according to Jenks natural breaks classification (Fig. 3). In these studies, it was concluded that the main issue was the lack of more precise data of past landslide occurrences.

A number of devastating flash floods happened in the last decade, when human and economic losses were huge [Peshevski *et al.*, 2017]. The losses were amplified by inappropriate land-use (such as construction in flood plains, rapid illegal urbanization in hazard zones and constricted river courses), incomplete and poorly maintained riverbeds and infrastructure, and increased erosion due to logging in forests. All these changes are altering the hydrological processes and regimes, increasing the risk of flash floods, landslides, river, rill, sheet and roadside erosion. This has resulted in an increase of the potential transported sediments, which more frequently reach built up areas in the transition to the Polog valley.

The last catastrophic event occurred on 3rd of August 2015 in the wider area of Tetovo town. Heavy rainfall was a trigger for flash flooding and a number of slope mass movements in the region (Fig. 4). Eleven settlements were affected by landslides, debris flows, earthflows or rock falls, which caused damages to infrastructure and structures, and unfortunately, casualities. There were 6 fatalities and 11 injuries; 24 families were evacuated from the Shipkovica settlement, 169 houses were directly flooded and 4 completely destroyed. The water supply systems in Tetovo, Shipkovica, Mala Golema Recica and Poroj were damaged. Eleven bridges and 17 roads were also damaged; additional six damaged bridges in Tetovo town and 1 in Jegunovce village. Furthermore, approximately 40 ha of agricultural land was flooded [Peshevski *et al.*, 2017]. This last event confirmed that landslides in the Polog Region present a significant natural hazard.

3. Landslide characterization by conventional methods

The conventional approach for landslide characterization used for the Polog Region consisted of several activities that were undertaken during a period of seven months, between November 2019 and June 2020. The main activities dealt with *i)* the analysis of own archive data on landslides and pho-

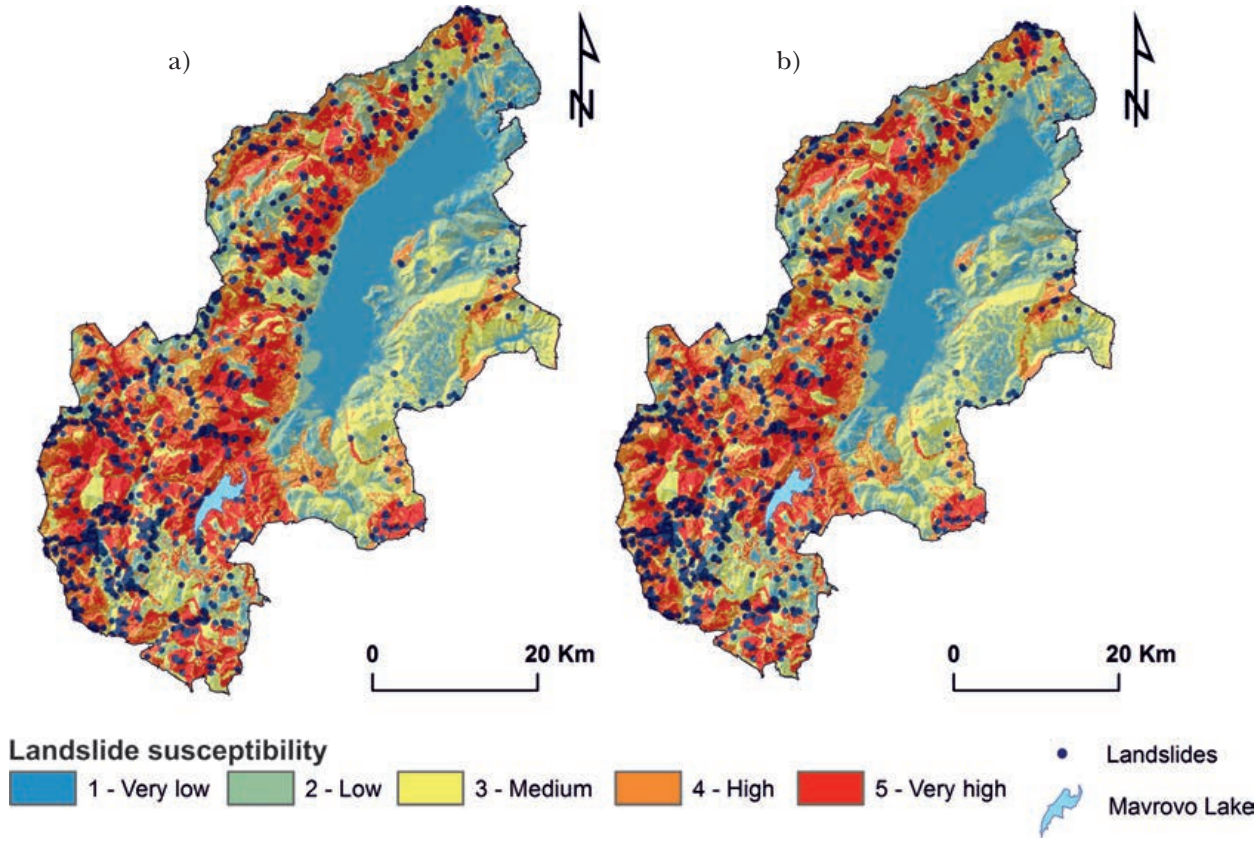

Fig. 3 – Landslide susceptibility map of Polog Region for return period of maximum expected seismic intensity for a) 100 years and b) 500 years (after PESHEVSKI *et al.*, 2019).

Fig. 3 – Carta della suscettibilità da frana della Regione Polog per un periodo di ritorno della massima intensità sismica attesa di a) 100 anni e b) 500 anni (modificato da PESHEVSKI et al.*, 2019).*

tointerpretation (performed in the period November 2019 - July 2020), *ii)* in-situ surveys to locations indicated by technicians of municipalities (from November 2019 to May 2020), *iii)* digitalization of landslide boundaries derived from available geological-geomorphological maps (at 1:25,000 scale) and from the archive of the Geological Survey of R.N. Macedonia (performed in the period December 2019 - March 2020), *iv)* interviews with employees and retired colleagues from geotechnical companies during the period November 2019 - January 2020, *v)* analysis of landslides along the channels of the "Mavrovo" system for hydro-energy production in June 2020, *vi)* in-situ surveys with colleagues from the National University in Tetovo in the period May - June 2020, *vii)* visits to several geotechnical companies in R.N. Macedonia in the period between November 2019-March 2020.

The landslide shape (body) for each single landslide was defined based on field mapping, morphology of the terrain, all available topographic maps. For some landslides, the analysis of a 2020 LiDAR survey for the region, with average density of point cloud of around 20 points per square meter and vertical accuracy less than 10 cm, was used. These accuracy characteristics of the point cloud data were considered sufficient for the purpose of regional landslide detection.

In this way, a landslide inventory with 136 occurrences was established. Then, in GIS environment, all phenomena were assigned the following data: location (*latitude, longitude, elevation, place name*), geology, and – where available – the landslide state of activity (*active, inactive, stabilized*), features (*type of movement, extension, direction of movement, trigger and depth*), and source of data.

The analysis of the results shed a light on several aspects. In particular, almost half of the landslides directly affected the population and the infrastructure network in the Polog Region, including disruption of the traffic flow and damage to the water channels of the "Mavrovo" hydro-system. For 24 landslides, damage was recorded; however, the detailed information on total losses is not available in the reports. Individual houses and settlements have been affected in 16 events. For 33 landslides, there is information on certain mitigation works, although the smaller interventions were probably not registered in any documentation.

As for the triggering factor(s) of landslide events, it was found that for most of the occurrences the fac-

Fig. 4 – Some photo of landslides and impacted infra(structures) during the last catastrophic event occurred on 3rd August 2015: a) debris fan near small electricity power plant; b) debris flow path through the Shipkovica village; c) debris flow material completely covering the road between Shipkovica and Brodec; d) affected area in Golema Recica.
Fig. 4 – Alcune foto di frane e infrastrutture/strutture coinvolte durante l'ultimo evento catastrofico del 3 agosto 2015: a) deposito detritico nei pressi di una piccola centrale elettrica; b) percorso della colata detritica attraverso il villaggio di Shipkovica; c) materiale della colata detritica che copre completamente la strada tra Shipkovica e Brodec; d) area colpita a Golema Recica.

tor is unknown (more than 60% out of the total). This is a limit and can lead to wrong conclusions during the preparation of landslide hazard maps. On the other hand, most of the remaining landslides resulted as rainfall-induced (Fig. 5a).

The type of sliding mechanism according to Cruden and Varnes [1996] is unknown almost for half of the landslides (Fig. 5b). For known cases, 40 occurrences were classified as translational slides, 8 complex slides, 13 rotational slides, 5 rockfalls, 3 rock avalanches, 1 snow-rock-tree avalanche and 1 rock slide. One landslide of flow type is registered in historical archives, or may be treated as floods events rather than flow-like slides. The only registered events of this type are those from the 2015 mass sliding events. However, this finding should be considered as a limiting factor from several aspects, especially for the selection of appropriate susceptibility (or hazard) method and calibration of such models.

The landslides were also classified according to the depth of the sliding surface, considering the value of 2.0 m of depth as a separation criterion between shallow and deep landslides [Cruden and Varnes, 1996; Hungr *et al.*, 2014; BRP/BWW/BUWAL, 1997]. Thus operating, it was found out that for half of the phenomena the depth of the sliding surface is unknown, 29 were classified as shallow landslides and 39 as deep landslides (Fig. 5d).

As for the state of activity, 37 landslides were considered active (Fig. 5c). The date of first activation of sliding and current state of activity is available for certain number of landslides, although some dates are only indicative (*i.e.* from verbal communication with municipality representatives). Previous data about landslide activity were very hard to obtain because of the lack of archives older than five-ten years. Finally, landslides were considered active if they exhibited movement in the last six months prior to the database creation. The number of detected inactive landslides is nine; whereas for 80 landslides the activity state is unknown. From the available documents, ten landslides were stabilized by control works; however, the number of remediated smaller landslides, for which unfortunately there aren't any records, is supposed to be much larger.

As far as the size of the landslide area is concerned, most of the landslides (55) were classified as large (10,000 – 100,000 m^2), 30 slides were classified

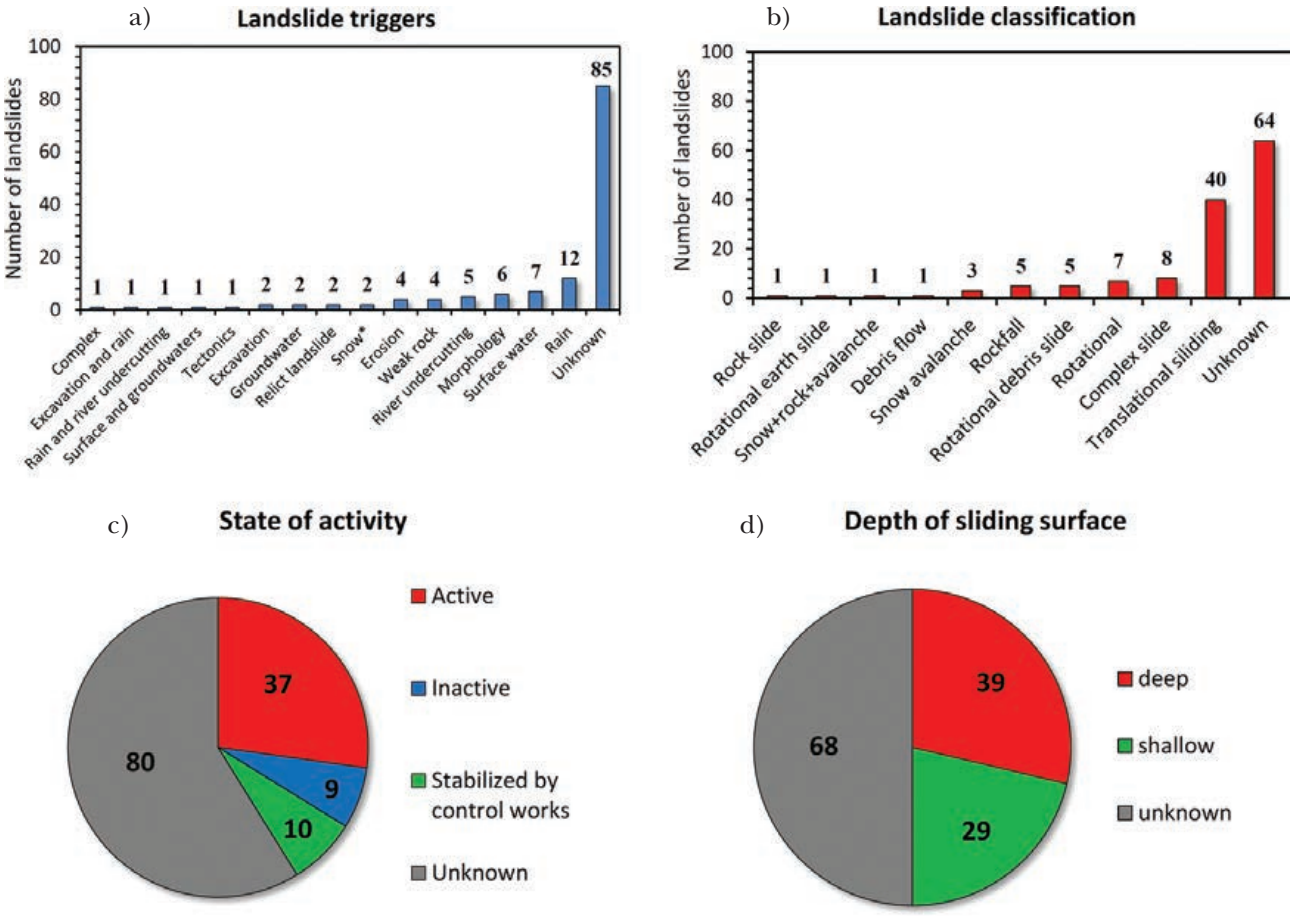

Fig. 5 – Landslides classification according to a) triggering factor ; b) type; c) state of activity; and d) depth of the sliding surface.

Fig. 5 – Classificazione delle frane in base a: a) fattore di innesco; b) tipologia; c) stato di attività e d) profondità della superficie di scorrimento.

as very large (> 100,000 m^2) and 27 of medium size (1000 – 10,000 m^2). Only four slides belong to the category very small (< 100 m^2) and seven slides were classified as small (100-1000 m^2). For the remaining 13 phenomena, information on the size is unknown.

With reference to the landslide movement direction, most landslides move in east north-east to south south-west direction.

The most important parameter controlling the distribution of landslides is the lithological composition of the terrain. Most landslides develop along the contact between debris and schist bedrock. The region is largely characterized by the presence of old tectonically affected Precambrian metamorphic complex, thus the terrain has a natural precondition for development of sliding processes.

Currently, the inventory consists of 136 mapped phenomena, and in time, it should be appropriately updated. The landslide inventory of the whole Polog study area is provided in figure 6a, whereas three close-up views to some landslides around urban settlements are given in figures 6a1, 6a2, 6a3.

4. Landslide characterization by DInSAR techniques

4.1. Image dataset and processing algorithm

The processing at the full spatial resolution was carried out over the whole Polog Region via the SAR Tomography technique [FORNARO *et al.*, 2014]. Similar to the Persistent Scatterer Interferometry (PSI) [FERRETTI *et al.*, 2001; COSTANTINI *et al.*, 2008], SAR Tomography operates at the full spatial resolution and allows monitoring ground objects also referred to as Persistent Scatterers (PS), *i.e.* targets characterized by a persistent electromagnetic response over the entire period of observation and from multiple orbits. It brings the imaging concept of the synthetic aperture in the slant-height (elevation) direction, orthogonal to the radar Line-of-Sight, based on the availability of multiple observations from slightly different orbits. This makes possible to focus at high resolution also in the third dimension (height) the signal backscattered from

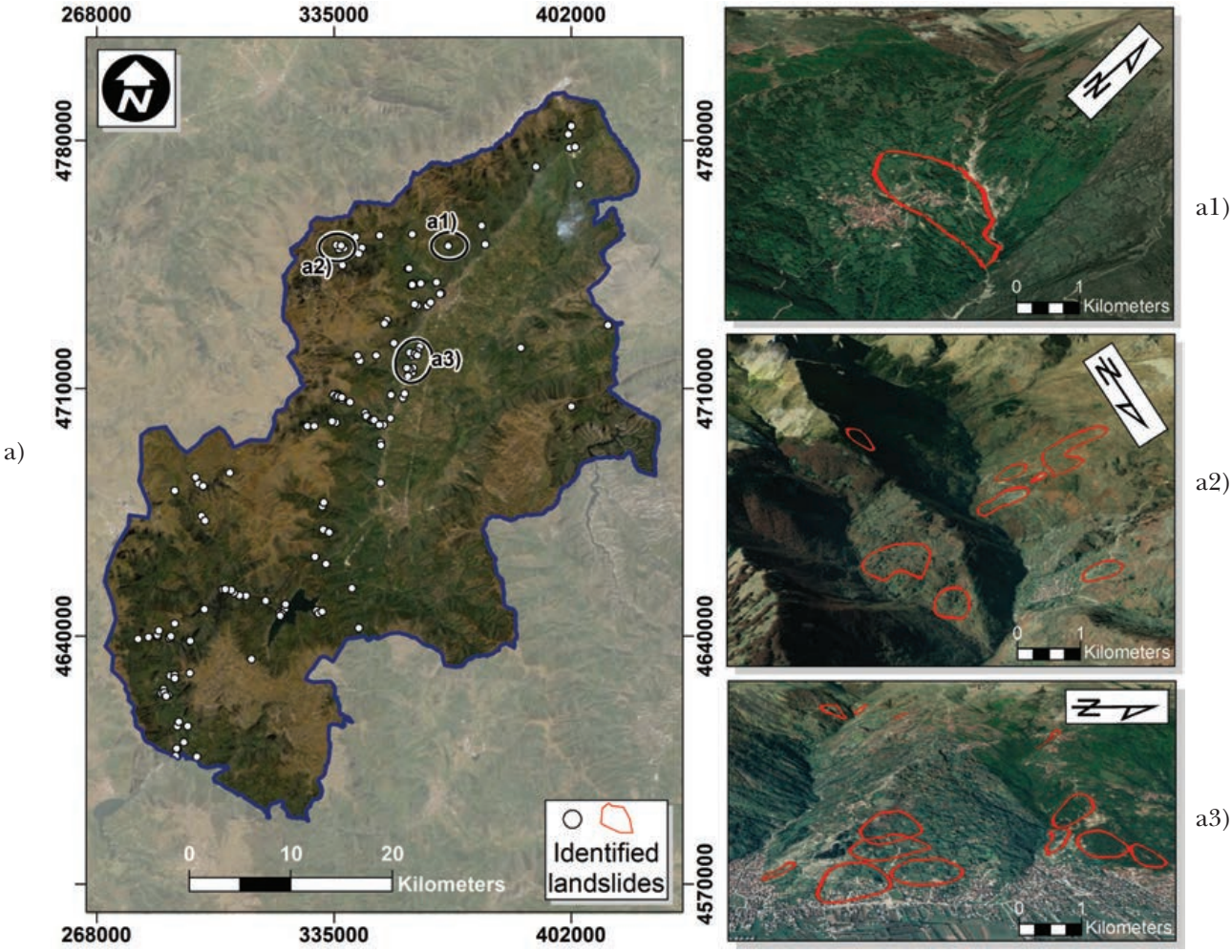

Fig. 6 – a) The current landslide inventory presented on a earth satellite imagery of the Polog Region with some close-up views: a1) Gjermo; a2) Bozovtse; and a3) landslides above Bogovinje and Kamenjane villages.
Fig. 6 – a) L'attuale inventario delle frane sovrapposto ad un'immagine satellitare della Regione Polog con alcuni zoom: a1) Gjermo; a2) Bozovtse e a3) frane nei villaggi di Bogovinje e Kamenjane.

ground objects, hence, the name 3D imaging. The imaging concept can be even further extended by including in the processing the possible temporal diversity of SAR multipass acquisitions, therefore extending the focusing in a space/velocity volume (4D imaging) to measure the deformation parameters of any temporal coherent PS in the focused 3D space. Monitoring capability can be pushed up to measure the slight movements induced by the thermal dilation of the imaged structures [FORNARO *et al.*, 2014]. Like PSI, SAR Tomography requires a strict phase calibration of the measured data aimed at compensating phase errors, mainly associated with propagation delays in the atmosphere of the electromagnetic radiation, which cause phases mismatch with the expected linear models associated with height and deformation contributions.

For the purpose of the present study, a set of 237 multipass SAR images acquired over ascending orbits by the Sentinel-1A and -B satellites of the European Space Agency, on relative orbit 175 within April 2015 to December 2019, was exploited. Based on the extent of the Polog Region with respect to the wide coverage of a single Sentinel-1 slice acquired in standard Interferometric Wide Swath (IW) acquisition mode, the processing has been limited to three bursts of the IW2 subswath.

The processing of the data was performed through the two-scale algorithm of FORNARO *et al.* [2014] that operates at different spatial scales: in a first stage, a Small-Baseline approach [BERARDINO *et al.*, 2002; FORNARO *et al.*, 2009] is implemented on spatially averaged data. The spatial averaging reduces the spatial resolution of the data to the order of tens to hundreds of meters. The processing on these low-resolution data allows estimating and compensating from the original acquisitions the phase contribution associated with the propagation of electromagnetic waves in atmosphere and possible deformation acting on a large scale.

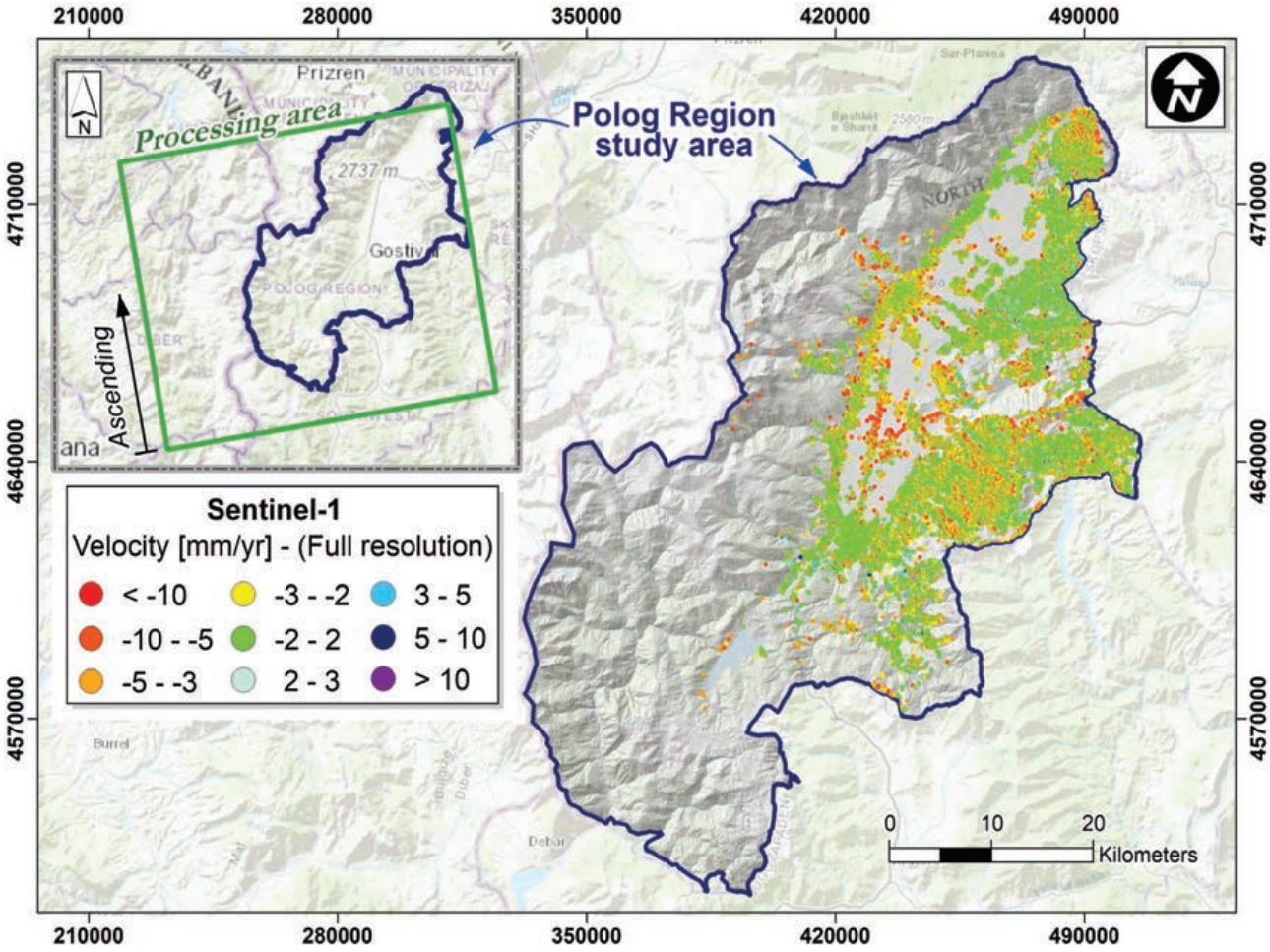

Fig. 7 – Spatial distribution of the DInSAR data velocity derived by the tomographic processing at full resolution (5m × 20m) of Sentinel-1 images acquired on ascending orbit over the Polog Region in the period spanning from 03/04/2015 to 29/07/2019.

Fig. 7 – Distribuzione spaziale delle velocità DInSAR derivate dalla elaborazione tomografica ad alta risoluzione (5m × 20m) delle immagini Sentinel-1 acquisite in orbita ascendente sulla Regione Polog nel periodo compreso tra il 03/04/2015 e il 29/07/2019.

This step is mandatory for the execution of the second, and most important, Tomographic processing at the full available spatial resolution of the data. For this study, a 4D Imaging (space/velocity) procedure has been implemented. The detection of reliable PS (*i.e.* the final test that allows determining the sparse map of output PS) has been implemented by exploiting a Generalized Likelihood Ratio Test (GLRT) scheme, which is based on the comparison of the normalized correlation among the measurement vector and the expected phase model with a threshold set according to the designed probability of false alarm. It has been demonstrated that such processing provides better performances in the detection of single PS and estimation of parameters of interest with respect to the classical PSI detector [DE MAIO *et al.*, 2009]. The map in figure 7 shows the spatial distribution of detected coherent targets with their average velocity along the sensor-target Line of Sight (LOS) referred to the period of observation. As expected, most of coherent targets concentrate on urbanized areas located in the plain. Some targets are also detected on the hillside that represents the focus of this analysis. Western part of the Polog Region, characterized by the presence of high mountains, is affected by severe decorrelation that causes lack of detected PS.

4.2. DInSAR data analysis

The analysis of DInSAR data pursued two main goals: the check of the inventoried landslides in terms of boundaries and state of activity, the detection of unmapped unstable sloping areas.

Referring to the study area, a check of the inventoried landslides in which at least one coherent DInSAR pixel was found within a buffer of 30 m drawn around the landslide boundaries (to take into account possible geolocalization errors) was carried out. Figure 8a

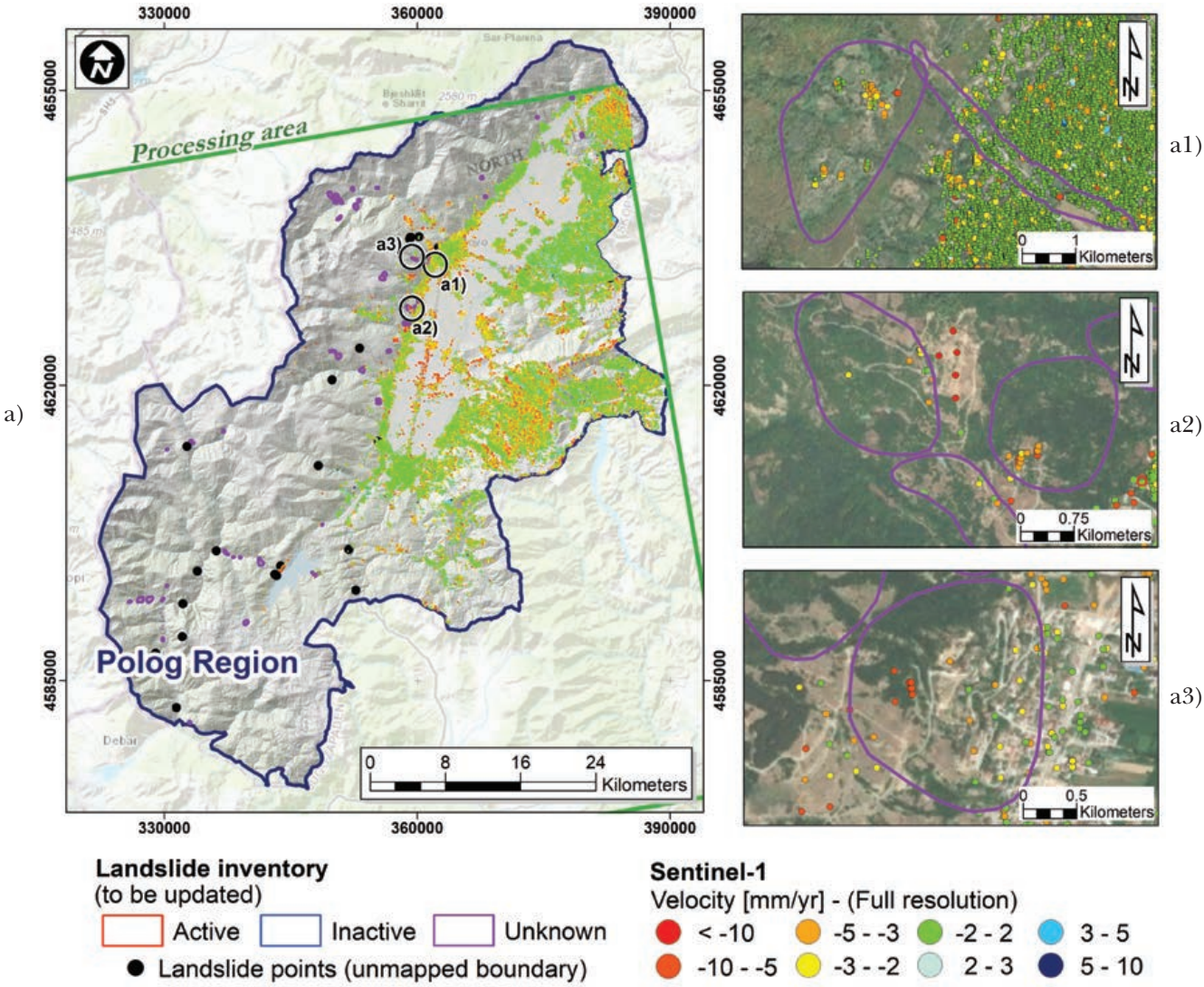

Fig. 8 – a)Map of detected PS derived from the tomographic processing of Sentinel-1 images spanning from 03/04/2015 to 29/07/2019 superimposed to the landslide inventory map of Polog Region with a1), a2), and a3) close-up views of some covered landslides.

Fig. 8 – a) Mappa dei PS derivata dall'elaborazione tomografica delle immagini Sentinel-1 dal 03/04/2015 al 29/07/2019 sovrapposta alla carta inventario delle frane della Regione Polog con a1), a2) e a3) viste ravvicinate di alcune frane coperte dai dati di interferometria satellitare.

shows the map of DInSAR coherent targets superimposed to the landslide inventory with three close-up views of some covered landslides (Figs. 8a1-a3). Twenty-four landslides out of a total of 136 resulted to be covered. Then, a further step of the analysis dealt with the selection of those coherent pixels exceeding a velocity threshold assumed as indicator of movement. This threshold was fixed equal to 2 mm/year [Cascini *et al.*, 2013; Peduto *et al.*, 2015]. In table I the state of activity (whether available) of mapped landslides distinguished per type is compared with the condition of "movement/no-movement" provided by DInSAR data along the sensor LOS.

Interestingly, only nine of the covered landslides were fully classified in the inventory in terms of type and state of activity. Accordingly, the analysis of DInSAR data could turn out useful to provide some insights into the kinematics of the abovementioned phenomena with reference to the period of observation of the available SAR images (03/04/2015 to 29/07/2019).

Unfortunately, because of strong decorrelation, southern part of the Polog Region is only partially covered by DInSAR data, as it can be seen in figures 7 and 8. In particular, only in the south-eastern portion – where no landslide polygons are present in the available inventory map – coherent benchmarks were retrieved by the SAR images processing. The density of points heavily reduces moving towards northwest, with no coherent benchmarks in the mountainous portion due to decorrelation effects.

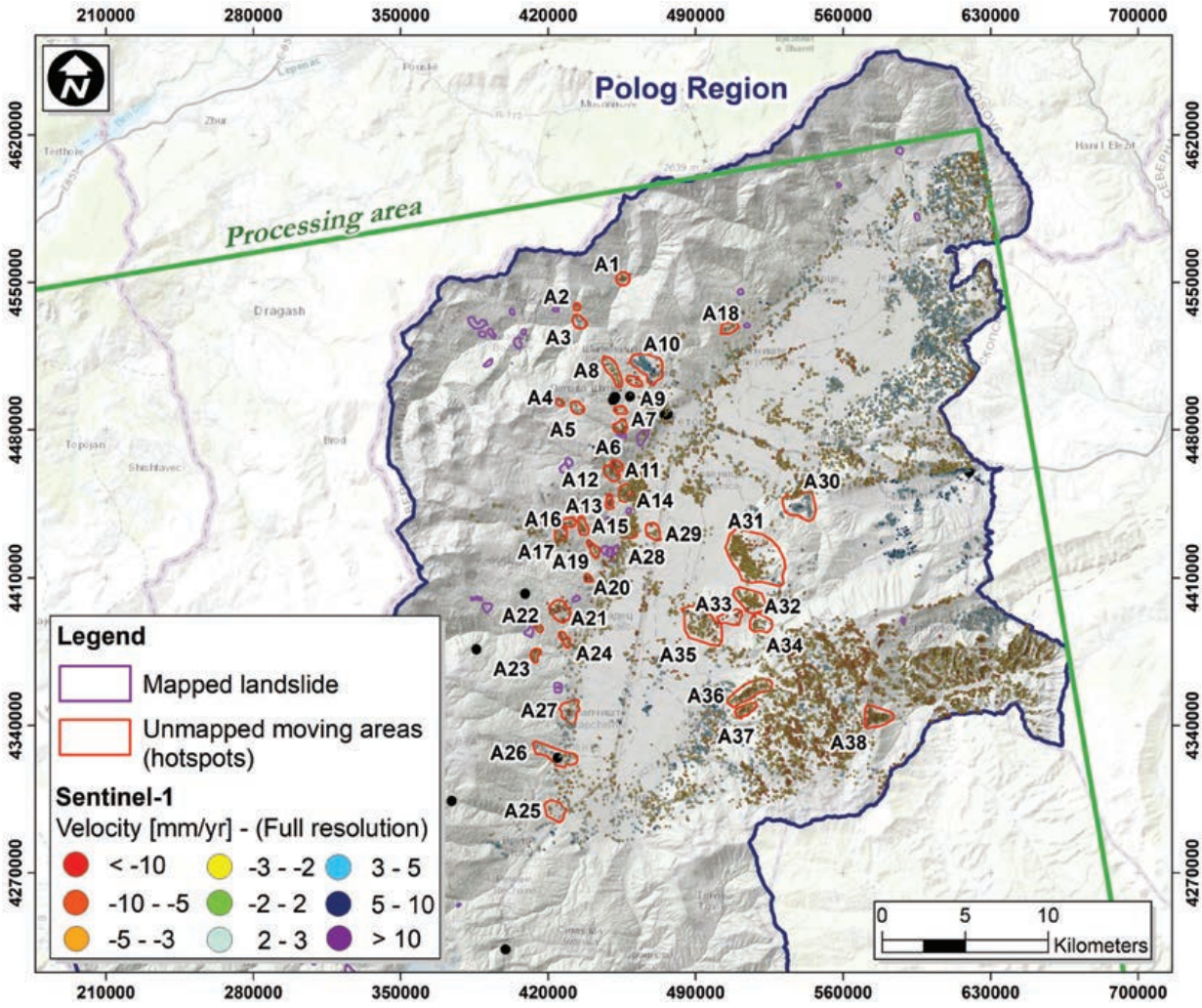

Fig. 9 – Map of hotspots identified using Sentinel-1 DInSAR data over Polog Region.
Fig. 9 – Mappa degli hotspot identificati utilizzando i dati DInSAR di Sentinel-1 sulla regione Polog.

As it is well-known in the scientific literature, DInSAR data besides contributing to landslide characterization (*e.g.*, definition of boundaries of landslide-affected areas; state of activity) can valuably complement with geomorphological criteria in landslide detection [PEDUTO *et al.*, 2021b]. This latter represented the second goal of DInSAR data analysis. For this purpose, based on the selected "moving coherent DInSAR pixels" over the whole Polog Region, 38 hotspots were identified, wherein a concentration of moving coherent pixels was identified out of the mapped landslides. These hotspots (Fig. 9) are mapped as areas that included at least 10 moving coherent DInSAR pixels and located on sloping areas (*i.e.* slope angle derived from the Digital Elevation Model greater than 5 degrees). This map could be exploited jointly with geomorphological/geological criteria and photointerpretation to map undetected landslides or to address in-situ surveys aimed at landslide reconnaissance.

Figures 10a and 10b show two examples of the hotspots identified over the study area as unmapped moving areas (called A10 and A20). The DInSAR coherent pixels homogeneously cover the two slopes that are densely urbanized. Considering the ascending orbit of the dataset at hand, the area seems to reveal an eastward movement with LOS DInSAR velocities ranging from 2 up to 10 mm/year. The current lack of (conventional) information on these areas may be related to the well-known difficulties of slow-moving landslide mapping in urban areas [GULLÀ *et al.*, 2017], wherein, conversely, DInSAR data provide the best monitoring performance and can be valuably coupled with the results of damage surveys to both buildings [BORRELLI *et al.*, 2018; DI MAIO *et al.*, 2018; PEDUTO *et al.*, 2021a,b] and roads [INFANTE *et al.*, 2018; NAPPO *et al.*, 2019]; unluckily, damage data are not yet available for the Polog Region. Therefore, in-situ and geomorphological investigations together with the analysis of crack patterns on structure/infrastructures will allow therein a deepening of knowledge on kinematics and on the "real" phenomena that affect the slopes.

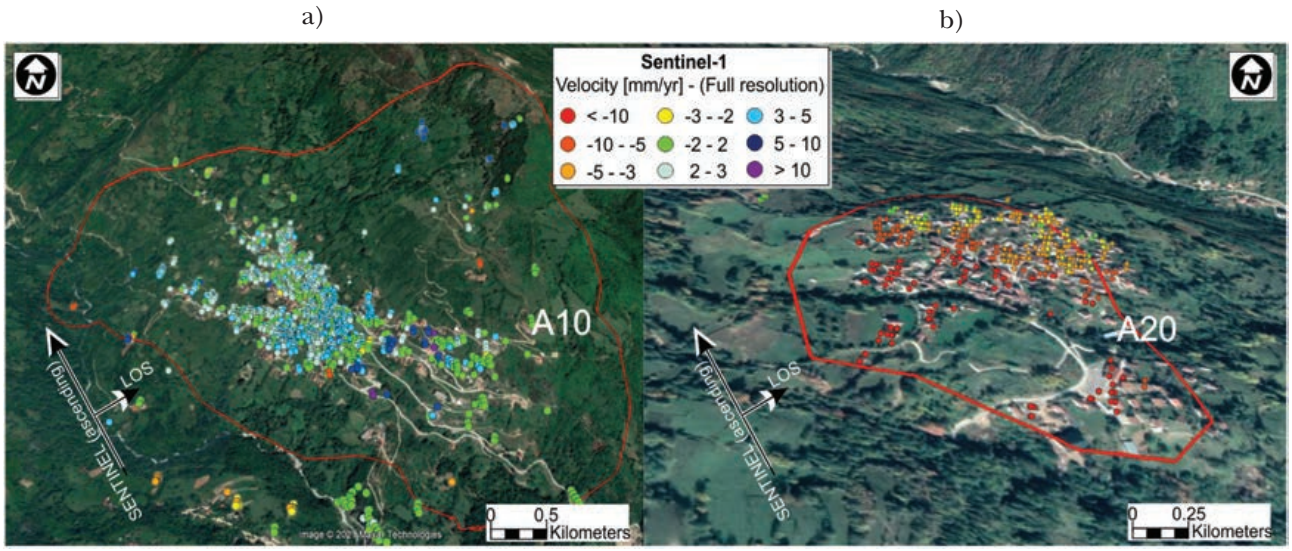

Fig. 10 – Examples of hotspots identified using Sentinel-1 DInSAR data: a) A10 and b) A20 reported in Fig. 9.
Fig. 10 – Esempi di hotspot identificati utilizzando i dati DInSAR di Sentinel-1: a) A10 e b) A20 indicati in Fig. 9.

5. Susceptibility maps for the Polog Region

Due to the lack of more precise data of past landslide occurrences, nonexistence of correlation between the landslide initiation with rainfall intensity, lack of data for flow-like type of movements, imprecise or missing data on landslide sediment produced during extreme events, the landslide assessment was developed at a susceptibility mapping level.

Based on the available data, two landslide susceptibility models were prepared for debris flow and shallow landslides. For this purpose, the following data

Tab. I – Type and state of activity of DInSAR-covered landslides with indication of the number of PS and measured LOS velocity.
Tab. I – Tipologia e stato di attività delle frane coperte dai dati DInSAR con indicazione del numero di PS e della velocità misurata lungo la LOS.

n.	ID	Type	State of activity	nr. PS	DInSAR average velocity [mm/year]			
					|min|	|max|	|avg.|	std. dev.
1	0	unknown	unknown	16	1.10	6.40	4.02	1.60
2	15	complex slide	unknown	7	4.70	38.0	9.10	13.63
3	27	unknown	unknown	2	0.60	1.80	1.20	1.20
4	28	unknown	unknown	110	0.40	16.40	2.77	38.05
5	32	unknown	unknown	9	0.50	2.80	1.96	0.81
6	33	unknown	unknown	2	0.80	2.40	1.60	0.82
7	35	unknown	unknown	4	0.10	7.00	2.90	3.06
8	36	unknown	unknown	19	1.30	7.70	2.79	2.40
9	1006	unknown	unknown	2	0.70	7.30	4.00	4.67
10	1007	unknown	unknown	3	0.00	2.40	0.80	2.20
11	1008	unknown	unknown	2	1.40	1.40	1.40	0.00
12	1009	unknown	unknown	2	1.30	1.30	1.30	0.00
13	1015	unknown	unknown	1	1.40	1.40	1.40	0.00
14	1020	unknown	unknown	3	1.10	4.30	2.93	1.67
15	1021	rock slide	active	2	2.80	3.40	3.10	0.42
16	1025	unknown	unknown	639	3.70	6.10	0.42	0.97
17	1026	rotational earth slide	active	2	0.80	1.30	1.05	0.35
18	1027	translational slide	active	3	1.10	7.40	4.13	3.16
19	1028	translational slide	active	1	5.90	5.90	5.90	0.00
20	1029	unknown	inactive	3	0.90	0.90	0.90	0.00
21	1044	intensive erosion	inactive	6	1.30	1.30	1.30	0.00
22	1048	translational slide	active	2	0.10	0.10	0.10	0.00
23	1053	translational slide	active	2	0.20	0.20	0.20	0.00
24	1054	translational slide	active	3	0.90	6.50	3.33	2.56

sources were used: basic geological map at 1:25,000 scale (1970-1980); landslide inventory; LIDAR survey of the study area; topographic map at 1:25,000 scale; orthophoto images; high resolution DEM with filtered vegetation; DEM derivatives (hillshade, slope, delineation of streams and roads); land-use map derived from the LIDAR (for residential area detection) and a report for wild damps provided by UNDP.

5.1. Debris flow modeling

A first step concerned debris flow modeling over the rugged terrain configuration of the Polog Region. Due to the complexity of the phenomenon, the variability of influential factors and uncertainty in parameters, a simplified model based on empirical or semi-empirical approach was adopted. For this purpose, the free available software Flow-R (https://www.flow-r.org/) was used. Importantly, owing to the lack of registered past debris-flow events there was no possibility to perform more exact analyses, and therefore, the produced debris-flow maps can be considered only as debris-flow susceptibility maps, rather than a "regular" hazard maps.

The following input data for modeling in Flow-R were used: DEM, flow accumulation, geology, lithology, landuse, source areas, plan curvature and others. The DEM is fundamental for both the source area delineation and the propagation assessment, and its quality is of major importance for the accuracy of the results. In the analysis, the mass and volume are not taken in consideration, because the exact amounts cannot be easily assessed for large regions due to the significant mass displacements that occur from erosion and deposition. However, in order to obtain some preliminary expected quantities in a case of extreme weather events, later on an empirical assessment of the possible debris flow generated sediment within the watersheds in Polog Region was performed.

The grid cells of each input dataset were classified as (1) favorable, when initiation is possible, (2) excluded, when initiation is unlikely, or (3) ignored, when no decision can be taken. Datasets were combined according to the rule: a cell is a source area if it is selected as favorable at least once, but never excluded.

Two types of algorithms were involved in the propagation assessment: spreading algorithms controlling the path and the spreading of the debris flows; and friction laws determining the run-out distance. Flow direction algorithms and persistence functions control the spreading. Several flow direction algorithms were implemented in the software, but for debris flow modelling the relevant are: Holmgren algorithm [Holmgren, 1994] and modified Holmgren algorithm [Horton *et al.,* 2013]. The persistence function aims at reproducing the behavior of inertia, and weights the flow direction based on the change in direction with respect to the previous direction [Gamma, 2000]. The run-out distance assessment is based on simple frictional laws. More precisely the kinetic energy of the cell is calculated based on the kinetic energy of the central cell, the change in the potential energy and the energy lost in friction.

The methodology for preparation of the Flow-R models within this study consisted of: preparation of a 10 m x10 m resolution DEM of the study area; generation of flow accumulation; preparation of the geology map and definition of the classes with potential for initiating debris flow; preparation of land-use map based on Corine Land Cover [CLC, 2018] inventory; and definition of classes with a potential for initiating debris flow.

During the setup of parameters and algorithms for debris flow modelling, the following were selected for propagation calculation: Calculation method – Quick energy based discrimination (recommended for debris flows); Spreading algorithm – direction algorithm – Holmgren exp=4.0 (recommended for debris flows); Spreading algorithm – inertial algorithm – weights – default; Energy calculation – friction loss function – travel angle 10 degree; Energy limitation – velocity < 14 m/sec.

As for the definition of precipitation thresholds, since for the region of interest there are no particular historical data, we had to rely on analysis of previous studies from other regions. Owing to similar conditions for the meteorological settings, a study from the French Alps (Barcelonnette Basin) was selected. Therein, the following rules of thumb had been defined: for debris flow initiation the rain intensity ranges from 2.7 to 30 mm/h, and the total duration of the event ranges from 1 to 7 hours [Remaître *et al.*, 2010]. According to this study, and in comparison with the available measured data from only two meteorological stations "Pozarane" and "Popova Sapka" in Polog Region, it could be concluded that all scenarios are possible. Therefore, it was considered that it was not logical to include the parameter "rainfall intensity" as "eliminatory" criteria for areas of the Polog Region.

In the first stage of the analysis all potential debris flow source areas were present, without applying the filter of lithological composition (geology) and land use. As a second step, the land-use layer as well as geology layer were exploited. After analyzing these two "eliminatory" layers, using engineering logics the final zones considered as susceptible to debris flows were delimited. The obtained debris flow susceptibility map is shown in figure 11. These findings should be considered with great precaution, revised and checked as more advanced stages of investigations/modeling proceed.

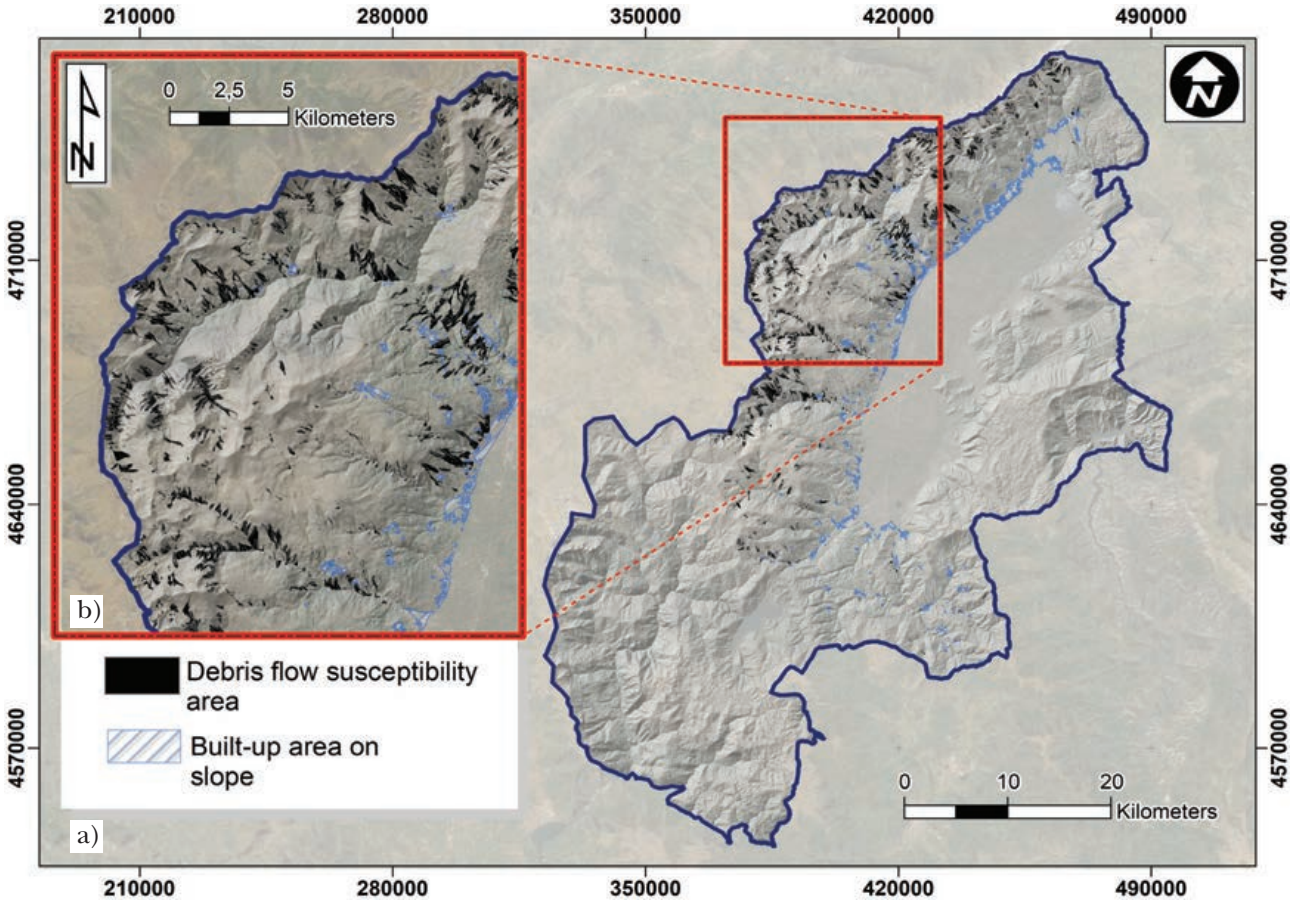

Fig. 11 – a) Preliminary debris flow susceptibility map and b) close-up view of northwest portion of Polog Region study area.
Fig. 11 – a) Mappa preliminare di suscettibilità da colata detritica e b) zoom sulla porzione nord-ovest dell'area di studio della Regione Polog.

5.2. Shallow landslide susceptibility assessment

Shallow landslides are typically translational sliding movements of soil material (earth and/or debris), characterized by a planar sliding surface in a depth of up to 2.0 m [Cruden and Varnes, 1996; Hungr *et al.*, 2014]. According to the Swiss recommendations (BRP/BWW/BUWAL 1997), landslides are classified as "shallow" if they are less than 2.0 m deep. Accordingly, based on the landslide inventory of the Polog Region, 21% of the landslides were confirmed in class of shallow landslides [Jovanovski *et al.*, 2021].

The infinite slope method [Skempton and DeLory, 1957] presented in figure 12 is a simple but very useful model for shallow sliding on a slip surface parallel to the slope of the ground, and it assumes that landslides are infinitely long but have small depth compared with their length and width. The infinite slope model has been used for analysis of shallow landslides in many studies [Alvioli *et al.*, 2014; Chae *et al.*, 2015; Chinkulkijniwat *et al.*, 2019; D'Amato *et al.*, 2009; Frattini *et al.*, 2004; Griffiths *et al.*, 2011; Lee and Park, 2015; Rosso *et al.*, 2006; Santoso *et al.*, 2011; Tsai *et al.*, 2015].

The infinite slope equation calculates a safety factor, based on limit equilibrium analysis that determines the balance between shear stress, which induces fracture along the supposed failure plane,

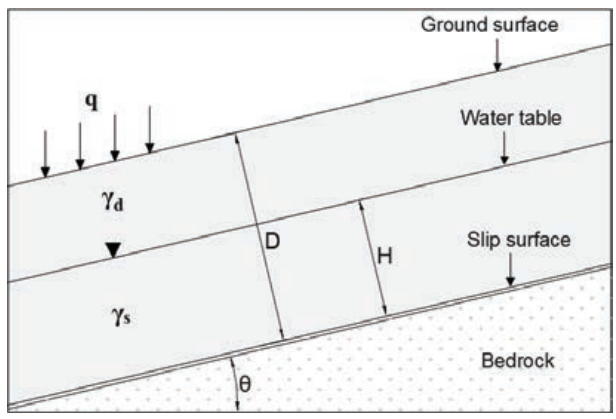

Fig. 12 – Schematic representation of the infinite slope method depicting the different parameters and variables (adapted from Skempton and DeLory 1957).
Fig. 12 – Rappresentazione schematica del modello di pendio indefinito raffigurante i diversi parametri e le variabili utilizzate (adattato da Skempton e DeLory 1957).

Tab. II – Input geotechnical parameters for the lithological units.
Tab. II – Parametri geotecnici di ciascuna unità litologica utilizzati come input per la modellazione.

Lithological unit	Unit weight of dry soil γ_d [kN/m^3]		Unit weight of saturated soil γ_s [kN/m^3]		Cohesion C_s [kN/m^2]		Angle of internal friction φ [°]	
	min	max	min	max	min	max	min	max
Alluvial sediments	17.0	18.6	20.0	21.6	0.0	16.0	20.0	36.0
Proluvial sediments	15.5	16.5	18.5	19.5	1.0	22.0	24.0	32.0
Diluvial and eluvial - diluvial sediments	16.0	18.5	19.0	21.5	10.0	30.0	25.0	29.0
Glacial and fluvioglacial sediments	14.0	16.0	17.0	19.0	8.0	20.0	22.0	32.0
Lacustrine sandy-clayey sediments	15.5	18.0	18.5	21.0	13.0	28.0	21.0	34.0

and shear strength, which serves to resist shear fracture. The following equation was used for calculation of the safety factor in this study, which was used by many other investigators [VAN WESTEN and TERLIEN, 1996; ACHARYA *et al.*, 2006; RAY and SMEDT, 2008]:

$$F = \frac{C_s + C_r}{\gamma_e D \sin\theta} + (1 - m\frac{\gamma_w}{\gamma_e})\frac{tan\varphi}{tan\theta}$$

wherein: F is slope safety factor (adimensional), Cs and Cr are effective soil and root cohesion (kN/m^2), D is soil depth above the failure plain (m), ϕ is angle of internal friction of the soil (^{0}), θ is slope angle (^{0}), γ_w is unit weight of water (kN/m^3), γ_e is effective unit weight of the soil (kN/m^3), and m is wetness index. VANWESTEN and TERLIEN [1996] define the effective unit weight, as:

$$\gamma_e = \frac{q cos\theta}{D} + (1 - m)\gamma_a + m\gamma_s$$

wherein: γ_d is unit weight of dry soil (kN/m^3), γ_s is unit weight of saturated soil(kN/m^3), and q is any additional load on the soil surface (kN/m^2).

The cohesion, dry and saturated unit weight and the friction angle of the soil (Tab. II) were determined from the available 1:200,000 scale engineering-geological map for Polog Region and from geotechnical reports of known landslides. The slope angle derived from the digital elevation model of the terrain (DEM), with grid size of 10×10 m. In order to estimate the soil depth above the failure plane the approach proposed by SAULNIER *et al.* [1997] was used. Many researchers have estimated the value of root cohesion for different vegetation species growing in different environments and CHOK *et al.* [2015] summarizes typical values of these. Considering the proposed values, as well as the forest cover information and land-use data for the Polog Region from CORINE, the representative values of root cohesion adopted in the analysis did not exceed 10kN/m^2 (*i.e.* for *coniferous forest* areas, see Tab. III). The parameter m, corresponding to the wetness index, theoretically expresses the relative position of the water H/D, where H is the saturated thickness of the soil above the failure plain and D is the total depth of the soil above the failure plain. Since the data at hand for calculation of the wetness index were very limited, three different scenarios of this value were assumed; namely, 0.35, 0.70 and 1.00.

Then, different stability classes were defined based on the values of the calculated safety factor (Tab. IV).

Several scenarios were analyzed for the Polog Region, in order to get a sense of the shallow landslide hazard/susceptibility in different saturation conditions and by taking in consideration the minimum and average values for the geotechnical strength parameters of the lithological units. Figure 13 shows the obtained shallow landslide susceptibility maps.

The obtained results suggest that shallow landslides are most likely to occur in the northernmost watersheds rather than in southern ones. If we consider the hypsometrical position of susceptibility zones in all the nine performed models, it is obvious that most landslides are expected to develop on the transition zone of the mountainous terrain towards the valley. Again, the northernmost part of the region is an exception because, therein, shallow landslides should be expected throughout the entire watersheds. The obtained results should undergo a critical review when more detailed data are collected for each separate watershed, *i.e.* in watershed level studies.

6. Discussion and conclusions

The preliminary landslide inventory, susceptibility maps and DInSAR data interpretation for the

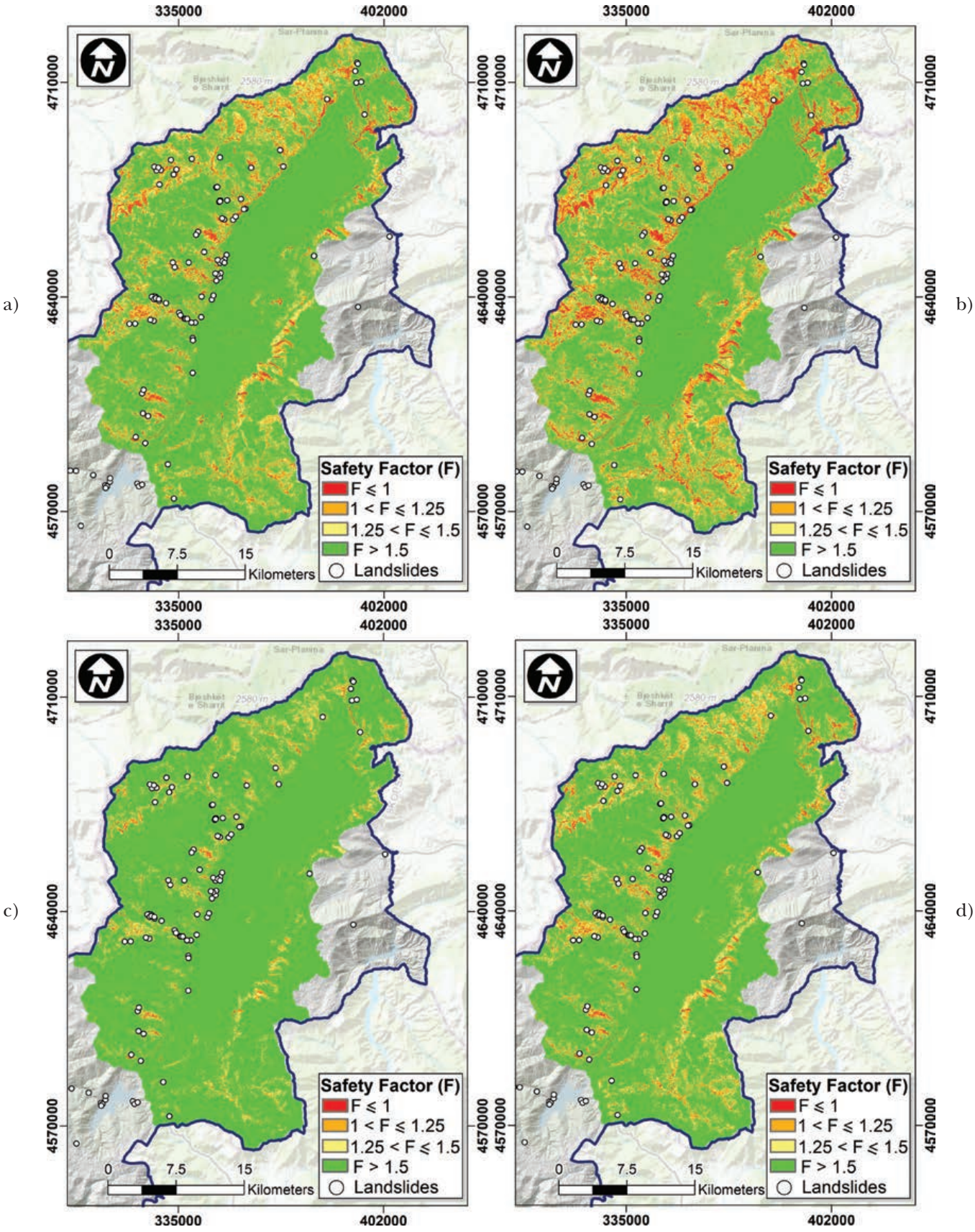

Fig. 13 – Shallow landslide susceptibility models for Polog Region: minimum values (Tab. II) of the geotechnical parameters with a) 35% and b) 70% soil saturation; average values (Tab. II) of the geotechnical parameters with c) 35% and d) 70% soil saturation.
Fig. 13 – Modelli di suscettibilità da frane superficiali per la Regione Polog: valori minimi (Tab. II) dei parametri geotecnici con a) 35% e b) 70% di grado di saturazione del suolo; valori medi (Tab. II) dei parametri geotecnici con c) 35% ed) 70% di grado di saturazione del suolo.

Tab. III – Root cohesion for land-use types and species in the Polog Region (adapted from CHOK *et al.*, 2015).
Tab. III – Valori del contributo coesivo delle radici assunti sulla base dell'uso del suolo e delle specie vegetali presenti nella Regione Polog (adattato da CHOK et al.*, 2015).*

n.	Land-use type	Cr [kN/m^2]
1	Discontinuous urban fabric	0.0
2	Industrial or commercial units	0.0
3	Mineral extraction sites	0.0
4	Non-irrigated arable land	0.0
5	Fruit trees and berry plantations	2.0
6	Pastures	2.0
7	Complex cultivation patterns	1.5
8	Land principally occupied by agriculture, with significant areas of natural vegetation	2.0
9	Broad-leaved forest	7.0
10	Coniferous forest	10.0
11	Mixed forest	2.0
12	Natural grasslands	0.0
13	Moors and heathland	2.0
14	Sclerophyllous vegetation	2.0
15	Transitional woodland-shrub	2.0
16	Sparsely vegetated areas	0.0
17	Burnt areas	0.0

Polog Region study area can be considered as satisfactory for this level of analysis (*i.e.* regional scale). Indeed, they represent sufficient background for the urging landslide management processes in the region. In particular, considering the almost total lack of information before the project started, the obtained results could help scientists and authorities in charge of land management to *i)* delimit zones/watersheds within the region that require more advanced study of the landslide hazards, *ii)* prioritize the landslides requiring detailed investigations and *iii)* those needing extensive monitoring.

In figure 14, the susceptibility maps were overlapped on both the landslide inventory and possible slow-moving sliding zones derived from DInSAR data analysis.

Depending on the type of landslide considered, it can be seen that the zones with highest susceptibility for shallow landslide occurrence match with most landslides from the inventory, suggesting the model is depicting quite well the real situation in the field. In relation to the assessment of flow-like events, it should be stressed that the adopted model is generally governed by the morphology of the terrain, while its verification is only possible after some time of data collection in an official database (which is suggested to be established as soon as possible for the region).

As most regional studies with basic level of landslide zonation, the following problems were

Tab. IV – Slope stability classes for the shallow landslide susceptibility model.
Tab. IV – Classi di stabilità assunte per il modello di suscettibilità da frane superficiali.

Safety factor	Slope stability class
F > 1.5	Stable
1.25 < F < 1.5	Moderately stable
1 < F < 1.25	Quasi stable
F < 1	Unstable

encountered during the course of the study. The shallow landslide model is limited by the availability of data related to soil thickness and relatively low number of data (and unevenly distributed in the region) for the geotechnical parameters of soils and the groundwater regime. The debris flow model is limited in relation to precipitation data, because only small number of data for rainfall intensities and durations is available. These were extrapolated for the entire region, which in reality is probably not the case. Furthermore, from the field surveys it was seen that the applied algorithm gives higher values of susceptibility for higher elevations, where the present rock types and weathering patterns are not indicating that such events had occurred very often in the recent past.

All these limitations should be overcome in more advanced studies, consisting of more detailed *in situ* geotechnical testing and sampling and monitoring of rainfalls, surface water regime and groundwater levels.

As for the identification of hotspots based on the analysis of DInSAR data, the joint analysis of the results of damage surveys to buildings and roads in the affected urban areas would be useful to confirm the existence of active landslides [NAPPO *et al.*, 2019; NOVIELLO *et al.*, 2020; PEDUTO *et al.*, 2017a; 2021b]. However, this aspect could be addressed more appropriately via the use of very high-resolution sensors, such as CosmoSkMed or TerraSarX, whose images unluckily are not available in a sufficient number for interferometric processing over the Polog Region. Notwithstanding, deepening on selected sites via the full-integration of DInSAR data with conventional monitoring and site-specific soil characterization will allow a further step toward slow-moving landslide analysis at the slope scale.

The proposed approach helps in the preliminary zonation of potential hazardous areas involving the local and regional authorities in charge of landslide risk management.

As the main achievement of the presented project, the exportation of the same procedure to other regions of R.N. Macedonia is envisaged. This is ex-

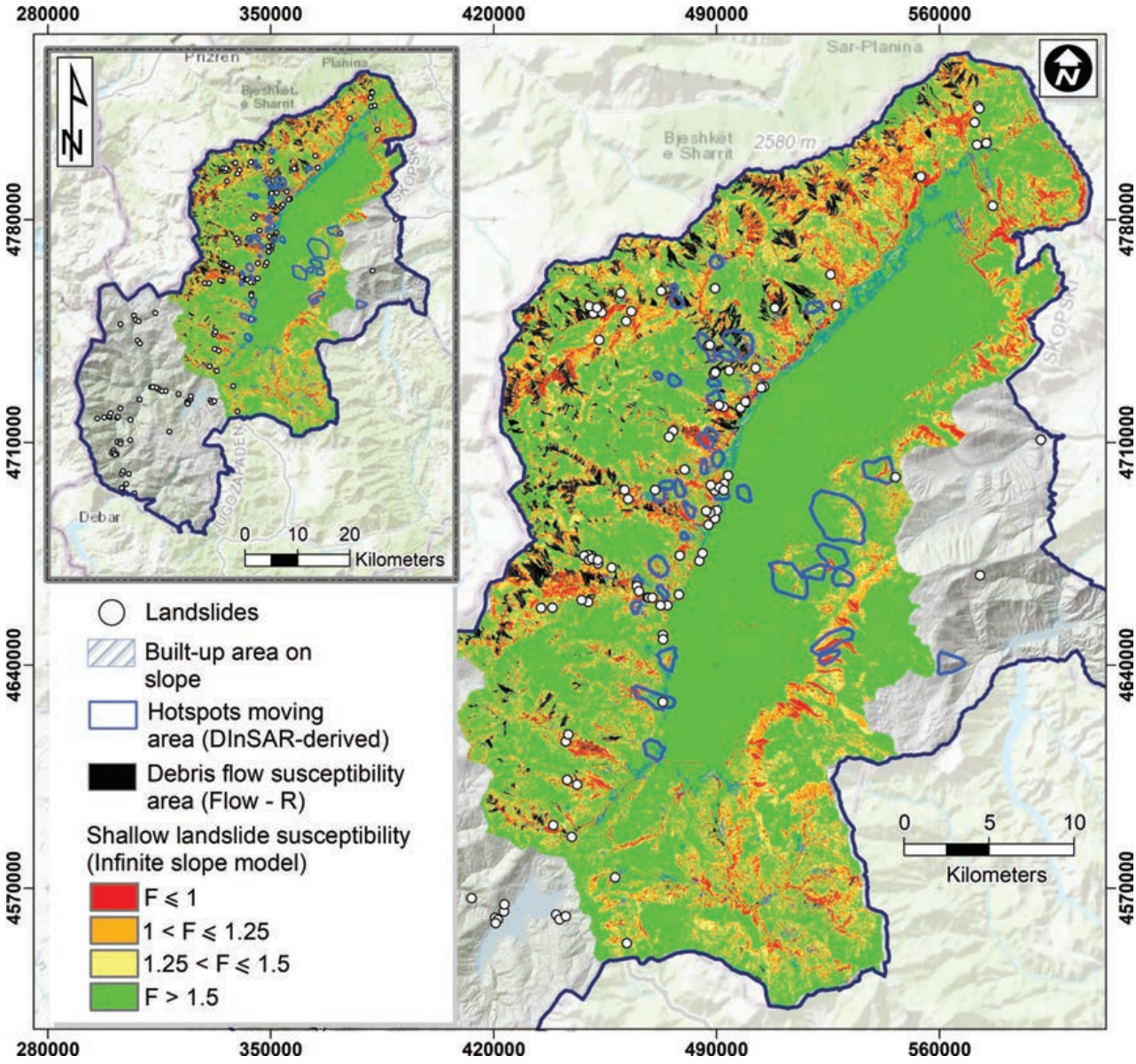

Fig. 14 – Landslide susceptibility zones in the Polog Region according to different methods.
Fig. 14 – Mappa delle aree suscettibili nella Regione Polog risultante dalla applicazione di metodologie differenti.

pected to play a key role in enriching the very limited available datasets as well as in fostering the improvement of natural disaster prevention in the country.

Acknowledgements

The present work was carried out within the Agreement For Research Funding between the Department of Civil Engineering of the University of Salerno (Italy) and the Faculty of Civil Engineering of the Ss. Cyril and Methodius University in Skopje (R.N. Macedonia) entitled: *Analysis and interpretation of remote sensing data (Differential Interferometric Synthetic Aperture Radar) for geotechnical studies pursuing the detection, mapping, and geometric and kinematic characterization of slope instabilities over the Polog Region (R.N. Macedonia).*

References

Abolmasov B., Milenkovic S., Jelisavac B., Radic Z. (2015) – *The analysis of landslide dynamicsbased on automated GNSS monitoring: a case study.* Engi. Geol. Soc. Territory Landslide Processes, 2, pp. 143-146.

Acharya G., De Smedt F., Long N.T. (2006) – *Assessing landslide hazard in GIS: a case study from Rasuwa, Nepal.* Bull. Eng. Geol. Environ., 65, n. 1, pp. 99-107.

Alvioli M., Guzzetti F., Rossi M. (2014) – *Scaling*

properties of rainfall induced landslides predicted by a physically based model. Geomorphology, 213, pp. 38-47.

Antronico L., Borrelli L., Peduto D., Fornaro G., Gullà G., Paglia L., Zeni G. (2013) – *Conventional and innovative techniques for the monitoring of displacements in landslide affected area.* In: C. Margottini (Ed.), Landslide science and practice, volume II: Early warning, instrumentation and monitoring. Springer, Berlin, pp. 125-131.

Antronico L., Borrelli L., Coscarelli R., Gullà G. (2015) –*Time evolution of landslide damages to buildings: the case study of Lungro (Calabria, Southern Italy).* Bull. Eng. Geol. Environ., 74, n. 1, pp. 47-59.

Arangio S., Calò F., Di Mauro M., Bonano M., Marsella M., Manunta M. (2013) – *An application of the SBAS-DInSAR technique for the assessment of structural damage in the city of Rome.* Structure and Infrastructure Engineering: Maintenance, Management, Life-Cycle Design and Performance 10, pp. 1469-1483.

Baldi P., Cenni N., Fabris M., Zanutta A. (2008) – *Kinematics of a landslide derived from archival photogrammetry and GPS data.* Geomorpholog., n. 102, pp. 435-444.

Bandini A., Berry P., Boldini D. (2015) – *Tunnelling-induced landslides: the Val di Sambro tunnel case study.* Eng. Geol., 196, pp. 71-87.

Barla G., Antolini F., Barla M., Mensi E., Piovano G. (2010) – *Monitoring of the Beauregard landslide (Aosta Valley, Italy) using advanced and conventional techniques.* Eng. Geol., 116, pp. 218-235.

Berardino P., Fornaro G., Lanari R., Sansosti E. (2002) –*A new algorithm for surface deformation monitoring based on small baseline differential SAR interferograms.* IEEE Trans. Geosci. and Remote Sens., 40, n. 11, pp. 2375-2383.

Bianchini S., Herrera G., Mateos R.M., Notti D., Garcia I., Mora O., Moretti S. (2013) – *Landslide activity maps generation by means of persistent scatterer interferometry.* Remote Sens, 5, pp. 6198-6222.

Bonci L., Calcaterra S., Cesi C., Gambino P., Gullà G., Niceforo D., Merli K., Sorriso-Valvo M. (2010) – *Displacements on a slope affected by deep-seated Gravitational Slope Deformation: Greci slope (Lago, Calabria, Italy).* Geogr. Fis. Din. Quat., 33, pp. 141-153.

Booth A.M., Dehls J., Eiken T., Fischer L., Hermanns R.L., Oppikofer T. (2015) – *Integrating diverse geologic and geodetic observations to determine failure mechanisms and deformation rates across a large bedrock landslide complex: the Osmundneset landslide, Sogn og Fjordane, Norway.* Landlsides, 12, pp. 745-756.

Borrelli L., Antronico L., Gullà G., Sorriso-Valvo G.M. (2014) – *Geology, geomorphology and dynamics of the 15 February 2010 Maierato landslide (Calabria, Italy).* Geomorphology, 208, pp. 50-73.

Borrelli L., Nicodemo G., Ferlisi S., Peduto D., Di Nocera S., Gullà G. (2018) – *Geology, slow-moving landslides, and damages to buildings in the Verbicaro area (north-western Calabria region, Southern Italy)* Journal of Maps, 14, n. 2, pp. 32-44, https://doi.org/10.1080/17445647.2018.1425164

Brp/Bww//Buwal (1997) – *Bundesamt für Raumplanung (BRP), Bundesamt für Wasserwirtschaft (BWW), Bundesamt für Umwelt, Wald und Landschaft (BUWAL) Berücksichtigung der Massenbewegungsge* – fahren bei raumwirksamen Tätigkeiten – Empfehlung, 42 pp.

Calò F., Calcaterra D., Iodice A., Parise M., Ramondini M. (2012) – *Assessing the activity of a large landslide in Southern Italy by ground-monitoring and SAR interferometric techniques.* Int. J. Remote Sens., 33, pp. 3512-3530.

Čarman M., Jemec Auflič M., Komac M. (2014) – *Landslides at a uranium mill tailing deposit site Boršt (Slovenia) detected by radar interferometry.* Landslides, 11, pp. 527-536.

Carter M., Bentley S.P. (1985) – *The geometry of slip surfaces beneath landslides: predictions from surface measurements.* Can. Geotech. J., 22, pp. 234-238.

Cascini L., Gullà G., Sorbino G. (2006) – *Groundwater modelling of a weathered gneissic cover.* Can. Geotech. J., 43, pp. 1153-1166.

Cascini L., Peduto D., Pisciotta G., Arena L., Ferlisi S., Fornaro G. (2013) –*The combination of DInSAR and facility damage data for the updating of slow-moving landslide inventory maps at medium scale.* Nat. Hazards Earth Syst. Sci., 13, pp. 1527-1549.

Chae B.-G., Lee J.-H., Park H.-J., Choi J. (2015) – *A method for predicting the factor of safety of an infinite slope based on the depth ratio of the wetting front induced by rainfall infiltration*, Nat. Hazards Earth Syst. Sci., 15, pp. 1835-1849, 2015 doi:10.5194/nhess-15-1835-2015

Chinkulkijniwat A., Tirametatiparat T., Supotayan C., Yubonchit S., Horpibulsuk S., Salee R., Voottipruex P. (2019) – *Stability characteristics of shallow landslide triggered by rainfall.* Journal of Mountain Science, 16, n. 9, pp. 2171-2183. https://doi.org/10.1007/s11629-019-5523-7

Chok Y.H., Jaksa M.B., Kaggwa W.S., Griffiths D.V. (2015) – *Assessing the influence of root reinforcement on slope stability by finite elements.* International Journal of Geo-Engineering 6, n. 12 (2015). https://doi.org/10.1186/s40703-015-0012-5

Ciampalini A., Cigna F., Del Ventisette C., Moretti S., Liguori V., Casagli N. (2012) – *Integrated geomorphological mapping in the north-western sector of Agrigento (Italy).* JOM, 8, pp. 136-145.

Cigna F., Osmanoglu B., Dixon T.H., De Mets C., Wdowinski, S. (2012) –*Monitoring land subsidence and its induced geological hazard with synthetic aperture radar interferometry: a case study in Morelia, Mexico.* Remote Sens. Environ., 117, pp. 46-161.

Corominas J., Van Westen C., Frattini P., Cascini L., Malet J.P., Fotopoulou S., Catani F., Van Den Eechaut M., Mavrouili O., Agliardi F., Pitilakis K., Winter M.G., Pastor M., Ferlisi S., Tofani V., Hervas J., Smith J.T. (2014) – *Recommendations for the quantitative analysis of landslide risk.* Bull. Eng. Geol. Environ., 73, n. 2, pp. 209-263.

Costantini M., Falco S., Malvarosa F., Minati F. (2008) –*A new method for identification and analysis of persistent scatterers in series of SAR image*s. In: IEEE International Geoscience & Remote Sensing Symposium, July 6-11, 2008, Boston, Massachusetts, USA, pp. 449-452.

Cotecchia F., Lollino P., Petti R. (2016) –*Efficacy of drainage trenches to stabilise deep slow landslides in clay slopes.* Géotechnique Lett., 6, n. 1, pp. 1-6.

Crosetto, M., Crippa, B., Biescas, E. (2005) – *Early detection and in-depth analysis of deformation phenomena by radar interferometry.* Eng. Geol., 79, pp. 81-91.

Cruden D.M., Varnes D.J. (1996) –*Landslide Types and Processes.* In: Turner, A.K., Schuster, R.L. (Eds.), *Landslides, Investigation and Mitigation*, Transportation Research Board Special Report 247, Washington D.C., pp. 36-75.

D'amato A.G., Falaschi F., Giannecchini R., Puccinelli A. (2009) – *Soil slip susceptibility assessment using mechanical-hydrological approach and GIS techniques: an application in the Apuan Alps (Italy*). Nat. Hazards., 50, n. 3, pp. 591-603.

De Maio A., Fornaro G., Pauciullo A. (2009) – *Detection of single scatterers in multidimensional SAR imaging.* IEEE Trans. Geosci. Remote. Sens., 47, n. 7, pp. 2284-2997.

Di Maio C., Vassallo R., Vallario M. (2013) – *Plastic and viscous shear displacements of a deep and very slow landslide in stiff clay formation.* Eng. Geol., 162, pp. 53-66.

Di Maio C., Fornaro G., Gioia D., Reale D., Schiattarella M., Vassallo R. (2018) – *In situ and satellite long-term monitoring of the Latronico landslide, Italy: Displacement evolution, damage to buildings, and effectiveness of remedial works.* Eng. Geol., 245, pp. 218- 235.

Eberhardt E. (2008) – *Twenty-ninth Canadian Geotechnical Colloquium: the role of advanced numerical methods and geotechnical field measurements in understanding complex deep-seated rock slope failure mechanisms.* Can. Geotech. J., 45, pp. 484-510.

Elias P., Kontoes C., Papoutsis I., Kotsis I., Marinou A., Paradissis D. And Sakellariou D. (2009) –*Permanent Scatterer InSAR Analysis and Validation in the Gulf of Corinth.* Sensors, 9, pp. 46-55.

Fell R., Corominas J., Bonnard C., Cascini L., Leroi E., Savage W.Z. (2008) – *Guidelines for landslidesusceptibility, hazard and risk zoning for land-use planning.* Eng. Geol., 102, nn. 3-4, pp. 99-111.

Ferlisi S., Marchese A., Peduto D. (2020) – *Quantitative analysis of the risk to road networks exposed to slow-moving landslides: a case study in the Campania region (Southern Italy).* Landslides, doi:10.1007/ s10346-020-01482-8

Ferretti A., Prati C., Rocca F. (2001) – *Permanent scatterers in SAR interferometry.* IEEE Trans. Geosci. Remote Sens., 39, n. 1, pp. 8-20.

Fornaro G., Pauciullo A., Reale D., Verde S. (2014) –*Multilook SAR tomography for 3-D reconstruction and monitoring of single structures applied to COSMO-SKYMED data.* IEEE J. Sel. Top. Appl. Earth Obs. Remote Sens., 7, n. 7, pp. 2776-2785.

Fornaro G., Reale D., Verde S. (2013) – *Bridge thermal dilation monitoring with millimeter sensitivity via multidimensional SAR imaging.* IEEE Geoscience and Remote Sensing Letters, 10, pp. 677-681. doi:10.1109/LGRS.2012.2218214

Fornaro G., Pauciullo A., Serafino F. (2009) – *Deformation Monitoring over Large Areas with Multipass Differential SAR Interferometry: a New Approach based on the Use of Spatial Differences*, Int. Journal of Remote Sens., 30, n. 6, pp. 1455-1478.

Frattini P., Crosta G.B., Fusi N., Dal Negro P. (2004) – *Shallow landslides in pyroclastic soils: a distributed modelling approach for hazard assessment.* Eng. Geol., 73, n. 3, pp. 277-295.

Galli M., Ardizzone F., Cardinali M., Guzzetti F., Reichenbach P. (2008) – *Comparing landslide inventory maps.* Geomorphology, 94, pp. 268-289. doi:10.1016/ j.geomorph.2006.09.023

Gamma P. (2000) – *Ein Murgang-Simulations program zur Gefahrenzonierung*, Geographisches Institut der Universität Bern, 2000 (in German).

Gili J.A., Corominas J., Ruis J. (2000) – *Using Global Positioning System techniques in landslide monitoring.* Eng. Geol., 55, pp. 167-192.

Grana V., Tommasi P. (2014) – *A deep-seated slow movement controlled by structural setting in marly formations of Central Italy.* Landslides, 11, pp. 195-212.

Griffiths D.V., Huang J.S., Fenton G.A. (2011) – *Probabilistic infinite slope analysis.* Comput. Geotech., 38, n. 4, pp. 577-584.

Gullà G., Peduto D., Borrelli L., Antronico L., Fornaro G. (2017) – *Geometric and kinematic characterization of landslides affecting urban areas: the Lungro case study (Calabria, Southern Italy).* Landslides, 14, n. 1, pp. 171-188.

Guzzetti F., Mondini A.C., Cardinali M., Fiorucci F., Santangelo M., Chang K.T. (2012) – *Landslide inventory maps: new tools for and old problem.* Earth-Sci. Rev., 112, pp. 42-66.

Hanssen F.R. (2003)–*Subsidence monitoring using contiguous and PS-INSAR: Quality assessment based on precision and reliability.* Proc. 11th FIG Symposium on Deformation Measurements, Santorini, Greece, pp. 1-8.

Haque U., Blum P., Da Silva P.F., Andersen P., Pilz J., Chalov R.S., Malet J.P., Jemec Auflič M., Andres N., Poyiadji E., Lamas C.P., Zhang W., Peshevski I., Pétursson G.H., Kurt T., Dobrev N,, García-Davalillo J.C., Halkia M., Ferri S., Gaprindashvili G., Engström J., Keellings D. (2016) – *Fatal landslides in Europe.* Landslides, 15, pp. 1545-1554.

Herrera G., Gutierrez F., Garcia-Davalillo J.C., Guerrero J., Notti D., Galve J.P., Fernandez-Merodo J.A., Cooksley G. (2013) – *Multi-sensor advanced DInSAR monitoring of very slow landslides: the Tena Valley case study (Central Spanish Pyrenees).* Remote Sens. Environ., 128, pp. 31-43.

Herrera G., Mateos R.M., García-Davalillo J.C., Grandjean G., Poyiadji E., Maftei, R., Filipciuc T.-C., Auflic M.J., Jež J., Podolszki L. (2018) – *Landslide databases in the Geological Surveys of Europe.* Landslides, 15, pp. 359-379.

Hervás J. (2013) – *Landslide inventory.* In: Encyclopedia of Natural Hazards, P.T. Bobrowsky (Eds.), Springer, Dordrecht, The Netherlands, pp. 610-611.

Holmgren P. (1994) – *Multiple flow direction algorithms for runoff modelling in grid based elevation models: An empirical evaluation.* Hydrological processes, 8, pp. 327-334.

Horton P., Jaboyedoff M., Rudaz B., Zimmermann M. (2013) – *Flow-R, a model for susceptibility mapping of debris flows and other gravitational hazards at a regional scale.* Nat. Hazards Earth Syst. Sci., 13, pp. 869-885

Hungr O., Leroueil S., Picarelli L. (2014) –*The Varnes classification of landslide types, an update.* Landslides, 11, n. 2, doi:10.1007/s10346-013-0436-y

Infante D., Di Martire D., Confuorto P., Tessitore S., Ramondini M., Calcaterra D. (2018) –*Differential SAR interferometry technique for control of linear infrastructures affected by ground instability phenomena.* International Archives of the Photogrammetry, Remote Sensing and Spatial Information Sciences, 42, n. 3, W4.

Infante D. Di Martire D., Confuorto P., Tessitore S., Tòmas R., Calcaterra D., Ramondini M. (2019) – *Assessment of building behavior in slow-moving landslide-affected areas through DInSAR data and structural analysis*, Engineering Structures, 199, 15 November 2019, n. 109638.

Ilijovski Z. (2013) – *Methodology for preparation of groundwater vulnerability maps.* Doctoral dissertation, Faculty of Civil Engineering, Skopje.

Jovanovski M., Radevski I., Peshevski I., Popovska C., Uzunov D., Peduto D. (2021) – *Feasibility study on basin-scale sediment management options for the Polog region.* Study funded by Swiss Agency for Development and Cooperation – SDC, implemented by UNDP as part of overall project: "Improving resilience to floods in Macedonia", Study prepared by Faculty of civil engineering, Skopje.

Komac M., Holley R., Mahapatra P., Van Der Marel H., Bavec M. (2015) – *Coupling of GPS/GNSS and radar interferometric data for a 3D surface displacement monitoring of landslides.* Landslides, 12, pp. 241-257.

Kjekstad O., Highland L. (2009) – *Economic and Social Impacts of Landslides.* Springer: Berlin/Heidelberg, Germany, pp. 573-587.

Lanari R., Reale D., Bonano M., Verde S., Muhammad Y., Fornaro G., Casu F., Manunta M. (2020) – *Comment on "Pre-Collapse Space Geodetic Observations of Critical Infrastructure: The Morandi Bridge, Genoa, Italy" by Milillo* et al. *(2019).* Remote Sensing, 12, n. 24, pp. 4011.

Lee J.-H., Park H.J. (2015) – *Assessment of shallow landslide susceptibility using the transient infiltration flow model and GIS-based probabilistic approach*, Landslides, October 2015 doi:10.1007/s10346-015-0646-6

Maiorano S.C., Borrelli L., Moraci N., Gullà G. (2015) – *Numerical modelling to calibrate the geotechnical model of a deep-seated landslide in weathered crystalline rocks: Acri (Calabria, Italy).* G. Lollino *et al.* (Eds.), Engineering Geology for Society and Territory, 2, pp. 1271-1274.

Massey C.I., Petley D.N., Mcsaveney M.J. (2013) – *Patterns of movement in reactivated landslides.* Eng. Geol., 159, pp. 1-19.

Merodo J.A.F., Davalillo J.C.G., Herrera G., Mira P., Pastor M. (2014) – *2D viscoplastic finite element modelling of slow landslides: the Portalet case study (Spain).* Landslides, 11, pp. 29-42.

Nappo N., Peduto D., Mavrouli O., Van Westen C.J., Gullà G. (2019) –*Slow-moving landslides interacting with the road network: Analysis of damage using ancillary data, in situ surveys and multisource monitoring data.* Engineering Geology, 260, https://doi.org/10.1016/j.enggeo.2019.105244

Nicodemo G., Ferlisi F., Peduto D., Aceto L., Gullà G. (2020a) –*Damage to masonry buildings interacting with slow-moving landslides: a numerical analysis.* In: F. Calvetti *et al.* (Eds). Proc. of the VII Italian Conference of Researchers in Geotechnical Engineering – CNRIG – Lecco, Italy 3-5 July, 2019, © Springer Nature Switzerland AG 2020, LNCE 40, pp. 52-61, https://doi.org/10.1007/978-3-030-21359-6_6

Nicodemo G., Peduto D., Ferlisi F. (2020b) –*Building damage assessment and settlements monitoring in subsidence-affected urban area: case study in The Netherlands.* Proc. of IAHS, © International Association of Hydrological Sciences, 382, pp. 651-656, https://doi.org/10.5194/piahs-382-651-2020

Nicodemo G., Peduto D., Ferlisi S., Maccabiani J. (2017) –*Investigating building settlements via very high resolution SAR sensors.* In: J. Bakker, *et al.* (Eds.), Life-Cycle of Engineering Systems: Emphasis on Sustainable Civil Infrastructure. Proc.

of the Fifth International Symposium on Life-Cycle Civil Engineering (IALCCE 2016), 16-19 October 2016, Delft, The Netherlands. Taylor & Francis Group, London, pp. 2256-2263, (ISBN 978-1-138-02847-0).

Noviello C., Verde S., Zamparelli V., Fornaro G., Pauciullo A., Reale D., Nicodemo G., Ferlisi S., Gullà G., Peduto D. (2020) –*Monitoring Buildings at Landslide Risk With SAR: A Methodology Based on the Use of Multipass Interferometric Data.* IEEE Geoscience and Remote Sensing Magazine (GRSM), MARCH 2020, 8, n. 1, pp. 91-119, doi: 10.1109/MGRS.2019.2963140

Pazzi V., Morelli S., Pratesi F., Sodi T., Valori L., Gambacciani L., Casagli N. (2016) –*Assessing the safety of schools affected by geo-hydrologic hazards: the geohazard safety classification (GSC).* Int. J. Disaster Risk Reduct., 15, pp. 80-93.

Peduto D, Cascini L, Arena L, Ferlisi S, Fornaro G, Reale D (2015) – *A general framework and related procedures for multiscale analyses of DInSAR data in subsiding urban areas.* ISPRS, J. Photogramm. Remote Sens., 105, pp. 186-210. ISSN 0924-2716, https:// doi.org/10.1016/j.isprsjprs.2015.04.001

Peduto D, Elia F, Montuori R (2018a) – *Probabilistic analysis of settlement-induced damage to bridges in the city of Amsterdam (The Netherlands).* Transport. Geotech., 14, pp. 169-182. https://doi.org/10.1016/j.trgeo.2018.01.002

Peduto D., Ferlisi S., Nicodemo G., Reale D., Pisciotta G., Gullà G. (2017a) – *Empirical fragility and vulnerability curves for buildings exposed to slow-moving landslides at medium and large scales,* Landslides, 14, n. 6, pp. 1993-2007, doi:10.1007/s10346-017-0826-7

Peduto D., Giangreco C., Venmans A.A.M. (2020) – *Differential settlements affecting transition zones between bridges and road embankments on soft soils: Numerical analysis of maintenance scenarios by multi-source monitoring data assimilation.* Transportation Geotechnics, 24, (2020) 100369.

Peduto D., Huber M., Speranza G., Van Ruijven J., Cascini L (2017b) – *DInSAR data assimilation for settlement prediction: case study of a railway embankment in The Netherlands.* Canadian Geotechnical Journal, 54, n. 4, pp. 502-517, http://dx.doi.org/10.1139/cgj-2016-0425

Peduto D, Korff M, Nicodemo G, Marchese A, Ferlisi S (2019a) – *Empirical fragility curves for settlement-affected buildings: analysis of different intensity parameters for seven hundred masonry buildings in The Netherlands.* Soils. Found., 59, n. 2, pp. 380-397, https:// doi.org/10.1016/j.sandf.2018.12.009

Peduto D., Nicodemo G., Cuevas-Gonzáles M., Crosetto M. (2019b) – *Analysis of damage to buildings in urban centres on unstable slopes via TerraSAR-X PSI data: the case study of El Papiol town (Spain).* IEEE Geoscience and Remote Sensing Letters, 16, n. 11), pp. 1706-1710, Print ISSN: 1545-598X, Online ISSN: 1558-0571, doi:10.1109/LGRS.2019.2907557

Peduto D., Nicodemo G., Maccabiani J., Ferlisi S. (2017c) – *Multi-scale analysis of settlement induced building damage using damage surveys and DInSAR data: a case study in The Netherlands.* Eng. Geol., 218, pp. 117-133.

Peduto D., Nicodemo G., Caraffa M., Gullà G. (2018b) – *Quantitative analysis of consequencesto masonry buildings interacting with slow-moving landslide mechanisms: a casestudy.* Landslides, 15, n. 10, pp. 2017-2030.

Peduto D., Oricchio L., Nicodemo G., Crosetto M., Ripoll J., Buxó P., Janeras M. (2021a) – *Investigating the kinematics of the unstable slope of Barberà de la Conca (Catalonia, Spain) and the effects on the exposed facilities by GBSAR and multi-source conventional monitoring.* Landslides, 18, pp. 457-469, https://doi.org/10.1007/s10346-020-01500-9

Peduto D., Santoro M., Aceto L., Borrelli L., Gullà G. (2021b) – *Full integration of geomorphological, geotechnical, A-DInSAR and damage data for detailed geometric-kinematic features of a slow-moving landslide in urban area,* Landslides, 18, pp. 807-825, https://doi.org/10.1007/s10346-020-01541-0

Peshevski I., Jovanovski M., Papic Br. J., Abolmasov B. (2015) – *Model for GIS landslide database establishment and operation in Republic of Macedonia.* Geological Macedonica, 29, n. 1, pp. 75-86.

Peshevski I., Peternel T., Jovanovski M. (2017) – *Urgent need for application of integrated landslide risk management stretegies for the Polog region in R. of Macedonia.* In: Advancing Culture of living with landslides. vol. V, Landslides in different environments, pp. 135-145, M. Mikos *et al.* (Eds.), Springer International Publishing 2017. doi:10.1007/978-3-319-53483-1_43

Peshevski I., Jovanovski M., Abolmasov B., Papić J., Marjanović M., Haque U., Nedelkovska N. (2019) –*Preliminary regional landslide susceptibility assessment using limited data.* Geologica Croatica, 72, n. 1, pp. 81-92.

Petkovski P. (1982) – *Basic geological map of Jugoslavia in scale 1:100 000, sheet Gostivar K34:78, map and interpreter.* Federal geological survey, Belgrade, pp. 75.

Petley D.N., Mantovani F., Bulmer M.H., Zannoni A. (2005) –*The use of surface monitoring data for the interpretation of landslide movement patterns.* Geomorphology, 66, pp. 133-147.

Pilot G. (1984) – *Instrumentation and warning system for research and complex slope stability problems.* Proc. 4th Int. Symp. on Landslides, Toronto, I, pp. 275-306.

Raspini F., Bianchini S., Ciampalini A., Del Soldato M., Montalti R., Solari L., Tofani V., Casagli, N. (2019) – *Persistent Scatterers continuous stream-*

ing for landslide monitoring and mapping: the case of the Tuscany region (Italy), Landslides, 16, n. 10, pp. 2033-2044.

RAUCOULES D., PARCHARIDIS I., FEURER D., NOVALLI F., FERRETTI A., CARNEC C., LAGIOS E., SAKKAS V., LE MOUELIC S., COOKSLEY G., HOSFORD S. (2008) – *Ground deformation detection of the greater area of Thessaloniki (Northern Greece) using radar interferometry techniques.* Nat. Hazards Earth Syst. Sci., 8, pp. 779-788.

RAY R.L., DE SMEDT F. (2008) – *Slope stability analysis on a regional scale using GIS: a case study from Dhading, Nepal.* Environ. Geol., (2009), 57, pp. 1603-1611.

REALE D., NITTI D.O., PEDUTO D., NUTRICATO R., BOVENGA F., FORNARO G. (2011) –*Postseismic deformation monitoring with COSMO/SKYMED constellation.* IEEE Geoscience and Remote Sensing Letters, 8, n. 4, pp. 696-700, ISSN 1545-598X.

REMAÎTRE A., MALET J.P., CEPEDA J. (2010) – *Landslides and debris flows triggered by rainfall: the Barcelonnette Basin case study, South French Alps.* In: J.-P. Malet, N. Casagli, T. Glade (Eds). Proc. of the International Conference "Mountain Risks: Bringing Science to Society", 24-26 November 2010. CERG Editions, Strasbourg, Firenze, Italy, pp. 141-146.

ROSSO R., RULLI M.C., VANNUCCHI G. (2006) – *A physically based model for the hydrologic control on shallow landsliding.* Water. Resour. Res., 42, n. 6, W06410. doi:10.1029/ 2005WR004369

SANABRIA M.P., GUARDIOLA-ALBERT C., TOMAS R., HERRERA G., PRIETO A., SANCHEZ H., TESSITORE S. (2014) – *Subsidence activity maps derived from DInSAR data: Orihuela case study.* Nat. Hazards Earth Syst. Sci., 14, pp. 1341-1360.

SANGIRARDI M., AMOROSI A., DE FELICE G. (2020) – *A coupled structural and geotechnical assessment of the effects of a landslide on an ancient monastery in Central Italy.* Engineering Structures, 225, pp. 111-249.

SANTOSO A.M., PHOON K.K., QUEK S.T. (2011) – *Effects of soil spatial variability on rainfall induced landslides.* Comput. Struct., 89, nn. 11-12, pp. 893-900.

SAULNIER G.M., BEVEN K.J., OBLED C. (1997) – *Including spatially variable effective soil depths in TOPMODEL.* J. Hydrol., 202, pp. 158-172.

SCHUSTER R.L., HIGHLAND, L. (2001) –*Socioeconomic and Environmental Impacts of Landslides in the Western Hemisphere.* Denver (CO) US Department of the Interior, US Geological Survey: Lakewood, CO, USA.

SKEMPTON A.W., DELORY F.A. (1957) – *Stability of natural slopes in London clay.* Proceedings 4th international Conference on Soil Mechanics and Foundation Engineering, 2, pp. 378-381.

STARK T.D., CHOI H. (2008) – *Slope inclinometers for landslides.* Landslides, 5, pp. 339.350.

TOFANI V., RASPINI F., CATANI F., CASAGLI N. (2013) – *Persistent Scatterer Interferometry (PSI) technique for landslide characterization and monitoring.* Remote Sens., 5, n. 3, pp. 1045-1065.

TOMÁS R., CANO M., GARCIA-BARBA J., VICENTE F., HERRERA G., LOPEZ-SANCHEZ J.M. (2013) – *Monitoring an earth fill dam using differential SAR interferometry: La Pedrera dam, Alicante, Spain.* Eng. Geol., 157, pp. 21-32.

TOMMASI P., PELLEGRINI P., BOLDINI D., RIBACCHI R. (2006) – *Influence of rainfall regime on hydraulic conditions and movement rates in the overconsolidated clayey slope of the Orvieto hill (Central Italy).* Can. Geotech. J., 43, pp. 70-86.

TSAI T.L., TSAI P.Y., YANG P.J. (2015) – *Probabilistic modelling of rainfall-induced shallow landslide using a point estimate method.* Environ. Earth. Sci., 73, n. 8, pp. 4109-4117.

VAN WESTEN C.J., TERLIEN T.J. (1996) – *An approach towards deterministic landslide hazard analysis in GIS: a case study from Manizales (Colombia).* Earth. Surf. Process. Landf., 21, pp. 853-868.

VAUNAT J., LEROUEIL S. (2002) – *Analysis of post-failure slope movements within the framework of hazard and risk analysis.* Nat. Hazards., 26, pp. 83-109.

WALSTRA J., DIXON N., CHANDLER J.H. (2007) – *Historic aerial photographs for landslide assessment: two case histories.* Q. J. Eng. Geol. Hydrogeol., 40, pp. 315-332.

WANG G., KEARNS T.J., YU J., SAENZ G. (2014) – *A stable reference frame for landslide monitoring using GPS in the Puerto Rico and Virgin Island region.* Landslides, 11, pp. 119-129

WASOWSKI J., BOVENGA F. (2014) – Inv*estigating landslides and unstable slopes with satellite multi temporal interferometry: current issues and future perspectives.* Eng. Geol., 174, pp. 103-138

YIN Y., ZHENG W., LIU Y., ZHANG J., LI X. (2010) – *Integration of GPS with InSAR to monitoring of the Jiaju landslide in Sichuan, China.* Landslides, 7, pp. 359-365

Caratterizzazione della franosità nella Regione Polog (R.N. Macedonia) con metodi innovativi e convenzionali

Sommario

L'articolo presenta i risultati preliminari di un progetto multidisciplinare internazionale finanziato dal Programma di sviluppo delle Nazioni Unite (UNDP) nella regione balcanica del Polog in R.N. Macedonia. Gli effetti combinati di un contesto geologico complesso, la morfologia articolata e le particolari condizioni climatiche fanno della Regione Polog una delle aree maggiormente esposte al rischio da frana nel Paese.

Sull'area di studio (con estensione di circa 1000 km^2) sono stati effettuati in passato studi preliminari di suscettibilità da frana; tuttavia, il quadro conoscitivo della franosità nella regione è ancora fortemente limitato dai pochi dati disponibili; pertanto, studi di maggiore dettaglio a copertura totale risultano necessari per l'analisi quali/quantitativa del rischio.

In tale contesto si inquadra il presente studio che persegue la rilevazione delle aree in frana e la analisi della loro interazione con il reticolo idrografico nella Regione al fine di proporre misure tecniche – a livello di studio di fattibilità – per le aree esposte al rischio più elevato.

Nella prima fase, attraverso il contributo congiunto di geologi/geomorfologi, idrologi, ingegneri geotecnici e idraulici, le attività si sono concentrate sulla preparazione di mappe tematiche delle sorgenti di sedimenti, tra le quali l'inventario delle frane gioca un ruolo di primaria importanza.

In via preliminare, le attività di base hanno riguardato i) l'analisi di carte geologiche e topografiche storiche e recenti, nonché rapporti tecnici su frane censite, ii) rilievi di campo e iii) raccolta di testimonianze di particolari eventi franosi.

I dati raccolti sono stati, quindi, analizzati in combinazione con dati da LIDAR (Light Detection and Ranging) aerotrasportato e misure di spostamento al suolo derivanti dal processamento mediante interferometria differenziale multipassaggio di immagini acquisite da radar satellitare ad apertura sintetica (DInSAR). Queste ultime sono state applicate per la prima volta in questa regione per l'analisi di pendii affetti da frane a cinematica lenta. Sono state condotte, inoltre, analisi preliminari di suscettibilità da frana in ambiente GIS con riferimento a fenomeni superficiali e debris flow.

L'approccio seguito si è rivelato adeguato ad un livello di studio di fattibilità in un'area come quella del Polog, dove la cartografia di base e tematica è incompleta o mancante. I risultati ottenuti hanno permesso i) una visione d'insieme, ancorché preliminare, delle condizioni di instabilità che interessano i versanti della Regione del Polog e ii) di individuare le aree a più elevata suscettibilità da frana. In tali aree, studi più approfonditi saranno condotti nelle fasi successive del progetto.